Pakistan Journal of Statistics and Operation Research

A New Model for Reliability Value-at-Risk Assessments with Applications, Different Methods for Estimation, Non-parametric Hill Estimator and PORT-VaRq Analysis

Mohamed Ibrahim[1,2*], Emadeldin I. A. Ali[3], G.G. Hamedani[4], Abdullah H. Al-Nefaie[2], Abdussalam Aljadani[5], Mahmoud M. Mansour[6,7], Haitham M. Yousof[7] , Mohamed S. Hamed[7,8] and Moustafa Salem[9]

* Corresponding Author

1. Department of Applied, Mathematical and Actuarial Statistics, Faculty of Commerce, Damietta University, Damietta, Egypt; mohamed_ibrahim@du.edu.eg
2. Department of Quantitative Methods, college of Business, King Faisal University, Al Ahsa 31982, Saudi Arabia; miahmed@kfu.edu.sa & aalnefaie@kfu.edu.sa
3. Department of Economics, College of Business, Al Imam Mohammad Ibn Saud Islamic University, Saudi Arabia; eiali@imamu.edu.sa
4. Department of Mathematical and Statistical Sciences, Marquette University, USA; gholamhoss.hamedani@marquette.edu
5. Department of Management, College of Business Administration in Yanbu, Taibah University, Al-Madinah, Al-Munawarah 41411, Kingdom of Saudi Arabia; ajadani@taibahu.edu.sa
6. Department of Management Information Systems, College of Business Administration in Yanbu, Taibah University, Madinah, Saudi Arabia; mmmansour@taibahu.edu.sa
7. Department of Statistics, Mathematics and Insurance, Benha University, Egypt; haitham.yousof@fcom.bu.edu.eg
8. Department of Business Administration, Gulf Colleges, KSA E-mail: mssh@gulf.edu.sa.
9. Department of Applied Statistics, Damanhour University, Egypt; moustafasalemstat@com.dmu.edu.eg

Abstract

This paper introduces a new extension of the exponential distribution tailored for enhanced reliability and risk analysis. We incorporate several insurance risk indicators like the value-at-risk, tail mean-variance, tail value-at-risk, tail variance, and maximum excess loss to significantly refine reliability risk assessments. These indicators offer vital insights into the financial consequences of extreme risk events and potential for substantial losses. To assess these risk indicators, we explore various non-Bayesian estimation techniques, including maximum likelihood estimation, ordinary least squares estimation, Anderson-Darling estimation, right tail Anderson-Darling estimation, and left tail Anderson-Darling estimation of the second order. Our approach involves a comprehensive simulation study with varying sample sizes, followed by empirical risk analysis using these methods. We also evaluate the applicability of the new model on two real reliability data sets. Finally, we apply the risk indicators including the value-at-risk (VaRq), tail mean-variance (TMVq), tail value-at-risk (TVaRq), tail variance (TVq) and maximum excess loss (MELq) to analyze reliability risk using failure (relief) and survival data. Finally the peaks over a random threshold value-at-risk (PORT-VaRq) analysis under the failure and survival data is presented.

Key Words: Characterizations; Extreme failure data; Key risk indicators; Risk analysis; Reliability; Threashold value-at-risk; PORT-VaRq.

1.Introduction

The exponential (E) distribution is widely used in risk analysis and reliability, but it has several limitations. First, it assumes a constant failure rate, which is unrealistic for many real-world systems where failure rates increase or decrease over time. Second, it lacks a memory property, meaning past failures do not influence future risk, making it unsuitable for aging systems. Third, it often underestimates the probability of extreme failures, leading to poor tail risk assessment. Fourth, it is inadequate for modeling systems with multiple failure modes, as real-world failures often follow more complex distributions. Fifth, it does not account for wear-out effects, making it inappropriate for many mechanical and electronic components. Sixth, it assumes failures are purely random, ignoring environmental and operational stress factors. Seventh, it may lead to over-simplified maintenance strategies, potentially increasing system risk. Eighth, alternative models like the Weibull or log-normal distributions often provide better accuracy in capturing real-world failure behaviors. This paper introduces a new exponential model designed to improve robustness in reliability risk analysis. It explores the integration of the risk indicators and applies various estimation methods to characterize the model's effectiveness. By delving into these elements, the paper aims to advance the field of reliability

engineering, offering refined tools and methodologies for more accurate and comprehensive risk management (see for more Bain (2017) details). These and other shortcomings represented the research gap that prompted us to present the extended exponentiated exponential (ExEE) distribution.

Starting with the exponentiated exponential (EE) distribution, a random variable (RV) X is said to have the EE distribution (see Gupta et al. (1998)) if its probability density function (PDF) is given by

$$g_{\mathrm{a,b}}(x)|(x>0,\mathrm{a}>0 \text{ and } \mathrm{b}>0)=\mathrm{ab}e^{-\mathrm{b}x}\left(1-e^{-\mathrm{b}x}\right)^{\mathrm{a}-1}. \tag{1}$$

The corresponding cumulative distribution function (CDF) can be written as

$$G_{\mathrm{a,b}}(x)|(x>0,\mathrm{a}>0 \text{ and } \mathrm{b}>0)=\left(1-e^{-\mathrm{b}x}\right)^{\mathrm{a}}. \tag{2}$$

Clearly, for $\mathrm{a}=1$, the EE reduces to the standard E model. If $1>\mathrm{a}$, the function $g_{\mathrm{a,b}}(X)$ monotonically decreases with x. If $\mathrm{a}>1$, the function $g_{\mathrm{a,b}}(X)$ attains a mode at $x=\frac{1}{\mathrm{b}}\log(\mathrm{a})$. The statistical properties of the EE model have been studied by many authors. Kamari and Alizadeh (2022) introduced a new flexible two parameters class of distributions extended type II exponentiated (ExII-G) family. Due to Kamari and Alizadeh (2022), the CDF of ExII-G is given by

$$F_{\alpha,\beta}(x)=\frac{1-[\bar{G}(X)]^{\alpha}}{1-[\bar{G}(X)]^{\alpha}+\overline{G}(X)^{\beta}}|(x\in R,\alpha>0 \text{ and } \beta>0), \tag{3}$$

where $\alpha,\beta>0$ and $\bar{G}(x)=1-G(x)$. The CDF of the ExEE distribution is given by

$$F_{\alpha,\beta,\mathrm{a,b}}(x)=\frac{1-\left[1-\left(1-e^{-\mathrm{b}x}\right)^{\mathrm{a}}\right]^{\alpha}}{1-[1-(1-e^{-\mathrm{b}x})^{\mathrm{a}}]^{\alpha}+[1-(1-e^{-\mathrm{b}x})^{\mathrm{a}}]^{\beta}}|(x>0,\alpha,\beta,\mathrm{a},\mathrm{b}>0), \tag{4}$$

where $x>0$, $\alpha>0$ and $\beta>0$ are two shape parameters. We denote it by ExEE $(\alpha,\beta,\mathrm{a},\mathrm{b})$. The PDF and HRF of ExEE are given by

$$f_{\alpha,\beta,\mathrm{a,b}}(x)=\mathrm{ab}e^{-\mathrm{b}x}\left(1-e^{-\mathrm{b}x}\right)^{\mathrm{a}-1}\left[1-\left(1-e^{-\mathrm{b}x}\right)^{\mathrm{a}}\right]^{\beta-1}\frac{\left\{\beta+(\alpha-\beta)\left[1-\left(1-e^{-\mathrm{b}x}\right)^{\mathrm{a}}\right]^{\alpha}\right\}}{\{1-[1-(1-e^{-\mathrm{b}x})^{\mathrm{a}}]^{\alpha}+[1-(1-e^{-\mathrm{b}x})^{\mathrm{a}}]^{\beta}\}^{2}}, \tag{5}$$

and

$$h_{\alpha,\beta,\mathrm{a,b}}(x)=\frac{\mathrm{ab}e^{-\mathrm{b}x}\left(1-e^{-\mathrm{b}x}\right)^{\mathrm{a}-1}\left\{\beta+(\alpha-\beta)\left[1-\left(1-e^{-\mathrm{b}x}\right)^{\mathrm{a}}\right]^{\alpha}\right\}}{[1-(1-e^{-\mathrm{b}x})^{\mathrm{a}}]\{1-[1-(1-e^{-\mathrm{b}x})^{\mathrm{a}}]^{\alpha}+[1-(1-e^{-\mathrm{b}x})^{\mathrm{a}}]^{\beta}\}^{2}}. \tag{6}$$

Recalling (4) and (5) and incorporating the insurance risk indicators such as VaRq, TMVq, TVaRq, TVq and MELq significantly enhances reliability risk analysis. These indicators provide crucial insights into the financial impacts of extreme risk events and the potential for large losses. The VaRq quantifies the maximum expected loss over a specified period with a given confidence level, while the TMVq and TVq assess the variability and potential for extreme outcomes in the tail of the distribution. TVaRq, on the other hand, focuses on the expected loss beyond a certain quantile, offering a more comprehensive view of risk (see McNeil and Saladin, (1997), Furman and Landsman (2006), Landsman (2010), and Mohamed et al. (2024)).

Moreover, following Alizadeh et al. (2024), the PORT-VaRq analysis is conducted under both failure and survival data scenarios. This method evaluates the distribution of extreme values exceeding a dynamic threshold, capturing tail risk behavior effectively. By applying this framework, the analysis identifies variations in risk exposure across different confidence levels. The increasing number of peaks as VaR decreases confirms the robustness of the tail risk assessment. Additionally, statistical measures such as the median, mean, and quartiles highlight the changing nature of extreme events over varying thresholds (see Alizadeh et al. (2024)). This approach provides a comprehensive understanding of risk concentration and the distribution of extreme financial events. Additionally, utilizing diverse estimation methods is essential for accurate risk assessment, particularly in calculating failure and survival times. Different approaches, such as maximum likelihood estimation, Bayesian methods, and non-parametric techniques, each provide unique insights and address various aspects of the data. Employing a range of estimation methods enables a more robust evaluation of risk, enhancing the precision and reliability of the analysis.

The characterizations of the (4), (5) and (6) based on two truncated moments, in terms of the hazard function and based on the conditional expectation of a function of the random variable are given with details. Alizadeh et al. (2017) present a comprehensive study on the generalized odd generalized exponential family of distributions. Hamedani et al. (2019) introduces the general exponential class of distributions, expanding the theoretical framework of exponential models. Korkmaz and Yousof (2017) explore the one-parameter exponential model, providing an in-depth analysis

of its mathematical properties and practical applications. In a follow-up to their previous work, Hamedani et al. (2018) investigate another general exponential class of distributions. Korkmaz et al. (2018b) present an exponential family of distributions. Goual et al. (2019) focus on validating the odd Lindley exponentiated exponential distribution using a modified goodness-of-fit test. Mansour et al. (2020b) propose a generalization of the reciprocal exponential model incorporating the Clayton copula. Bhatti et al. (2022) explore a new moment exponential distribution, focusing on its properties and applications. Yadav et al. (2021) investigate the Burr-Hatke exponential distribution, which features a decreasing failure rate model. Eliwa, El-Morshedy et al. (2022) introduce the discrete exponential family of distributions, presenting both Bayesian and non-Bayesian estimators. Yadav et al. (2022) validate the xgamma exponential model using the Nikulin-Rao-Robson goodness-of-fit test. Saber et al. (2022) discusses reliability estimation for the remained stress-strength model under the generalized exponential lifetime distribution. Minkah et al. (2023) address robust extreme quantile estimation for Pareto-type tails through an exponential regression model. Their study contributes to the understanding of extreme value estimation, offering methods for handling robust quantile estimation in extreme value analysis. Many other works presented useful extension with application such as Zheng (2002), Alizadeh et al. (2023a,b and 2025), Zheng and Park (2004), Kundu and Pradhan (2009), Aslam et al. (2010).

For assessing the risk indicators, we focus on non-Bayesian estimation techniques, examining some distinct methods to provide a broad perspective on their applications and effectiveness. Among these methods, we highlight maximum likelihood estimation (MLE), ordinary least squares estimation (OLSE), Anderson-Darling estimation (ADE), right tail Anderson-Darling estimation (RTADE), and left tail Anderson-Darling estimation of the second order (LAD 2) methods. First, we presented a comprehensive simulation method under different sample sizes. Second, an empirical risk analysis is presented under these selected methods. Third, the applicability on the new model is checked under two real reliability data sets. Finally, reliability risk analysis is provided using the VaRq, TMVq, TVaRq and TVq under the failure (relief) and survival data. For heavy-tailed distributions, the survival function often behaves asymptotically as

$$S_{\alpha,\beta,\mathrm{a},\mathrm{b}}(x) \approx x^{-\frac{1}{\mathbb{T}}},$$

where $\mathbb{T}$ is the tail index. To determine the tail index, we analyze the asymptotic behavior of $S_{\alpha,\beta,\mathrm{a},\mathrm{b}}(x)$ as $x \to \infty$. For the exponential-type distributions, it is known that their tail is light, meaning they decay exponentially rather than following a power law. Thus, the ExEE distribution does not have a heavy tail, and its tail index $\mathbb{T}$ is zero (or approaches zero), meaning the decay is exponential rather than polynomial. This means that the ExEE distribution does not belong to the class of distributions with regularly varying tails (such as Pareto, Fréchet, or other heavy-tailed models). Since the ExEE distribution decays exponentially, it does not belong to the class of distributions with regularly varying tails, such as the Pareto or Fréchet distributions. The Hill estimator will be zero or very close to zero, reinforcing this result.

The paper is organized as follows: Section 2 introduces and explores the fundamental properties of the new exponential distribution extension, detailing its mathematical characteristics. Section 3 derives and discusses specific characterizations of the model, providing theoretical foundations and proofs. Section 4 evaluates various assessment methods, comparing their effectiveness and suitability for different types of data. Section 5 presents results from simulation studies, illustrating the model's behavior under varying conditions. Section 6 provides an empirical risk analysis using real data to validate the model's practical applicability. Section 7 examines the model's applicability in diverse contexts, highlighting its flexibility and generalizability. Section 8 applies the model to reliability and risk analysis in dialysis, demonstrating its relevance to healthcare settings. The paper concludes by synthesizing findings from theoretical, empirical, and practical applications in Section 9.

2. Some properties

Due to Kamari and Alizadeh (2022), the PDF of the ExEE model can be expressed as

$$f_{\alpha,\beta,\mathrm{a},\mathrm{b}}(x) = \sum_{k=0}^{\infty} C_k \, g_{\mathrm{a}k,\mathrm{b}}(x), \tag{7}$$

where $g_{\mathrm{a}k,\mathrm{b}}(x) = \mathrm{a}k\mathrm{b}e^{-\mathrm{b}x}\left(1-e^{-\mathrm{b}x}\right)^{\mathrm{a}k-1}$, $C_0 = 1 + \mathrm{b}_0 | k = 0$, $C_k = \mathrm{b}_k | k \geq 1$ and b_k is given with details in Kamari and Alizadeh (2022). The r^{th} ordinary moment of X is given by $\mu'_r = E(X^r) = \int_{-\infty}^{\infty} x^r f(x)dx$, then we obtain

$$\mu'_{r}|r > -1 = \mathrm{b}^{-r}\Gamma(1+r)\sum_{k,v=0}^{\infty} C_{k,v}^{(\mathrm{a}k,r)}, \tag{8}$$

where

$$C_{k,v}^{(\mathrm{a}k,r)} = \mathrm{a}kC_k(-1)^v\frac{1}{(v+1)^{r+1}}\binom{\mathrm{a}k-1}{v},$$

and $\Gamma(1+\Delta)|\Delta \in R^+ = \Delta! = \prod_{r=0}^{\Delta-1}(\Delta - r)$ where $E(X) = \mu'_1$ is the mean of X. The r^{th} incomplete moment, say $I_r(-\infty, t)$, of x can be expressed, from (9), as

$$I_r(-\infty,t) = \int_{-\infty}^{t} x^r f(x)dx = \sum_{k=0}^{\infty} C_k \int_{-\infty}^{t} x^r g_{\mathrm{a}k,\mathrm{b}}(X)dx,$$

then

$$I_r(-\infty,t)|_{(r>-\delta)} = \mathrm{b}^{-r}\gamma(r+1,\mathrm{b}t)\sum_{k,v=0}^{\infty} C_{k,v}^{(\mathrm{a}k,r)}, \tag{9}$$

where $\gamma(\Delta,\varsigma)$ is the incomplete gamma function.

$$\gamma(\Delta,\varsigma)|_{(\Delta\neq 0,-1,-2,\ldots)} = \int_0^{\varsigma} exp(-x)\,dx = \frac{1}{\Delta}\varsigma^{\Delta}\{F_{1,1}[\Delta;\Delta+1;-\varsigma]\},$$

and $F_{1,1}[\cdot,\cdot,\cdot]$ is a confluent hypergeometric function. The first incomplete moment given by (11) with $r = 1$ as

$$I_1(-\infty,t) = \mathrm{b}\gamma\left(2,\frac{1}{t}\right)\sum_{k,v=0}^{\infty} C_{k,v}^{(1,\mathrm{a}k)}.$$

The MGF $M_X(t) = E(exp(tX))$ of X can be derived from equation (8) as $M_X(t) = \sum_{k=0}^{\infty} C_k M_{\mathrm{a}k,\mathrm{b}}(T)$, where $M_{\mathrm{a}k,\mathrm{b}}(T)$ is the MGF of the EE model with power parameter $\mathrm{a}k$

$$M_X(t)|r > -1 = \sum_{r=0}^{\infty}\sum_{k,v=0}^{\infty}\frac{t^r}{r!}\mathrm{b}^{-r}\Gamma(1+r)C_{k,v}^{(\mathrm{a},r)}. \tag{10}$$

The s^{th} moment of the residual life of X is given by

$$A_s(t,+\infty) = \frac{1}{1-F_{\alpha,\beta,\mathrm{a},\mathrm{b}}(t)}\int_t^{\infty}(x-t)^s\,dF(X).$$

Therefore,

$$A_s(t,+\infty) = \frac{1}{1-F_{\alpha,\beta,\mathrm{a},\mathrm{b}}(t)}\sum_{k,v=0}^{\infty} C_{k,v}^{(\mathrm{a}k,s)}\,\mathrm{b}^s\Gamma(s+1,\mathrm{b}t)|s > -1, \tag{11}$$

where

$$C_{k,v}^{(\mathrm{a}k,s)} = C_k\sum_{r=0}^{s}(-t)^{s-r}\binom{s}{r}, \Gamma(\Delta,r)|_{r>0} = \int_r^{\infty} x^{\Delta-1}\,exp(-x)\,dx$$

and $\Gamma(\Delta,r) = \Gamma(\Delta) - \gamma(\Delta,r)$. The s^{th} moment of the reversed residual life, say

$$A_s(0,t) = E[(t-Z)^s \mid x \le t, t > 0 \text{ and } s = 1,2,\ldots]$$

uniquely determines $F_{\alpha,\beta,\mathrm{a},\mathrm{b}}(x)$. We obtain

$$A_s(0,t) = \frac{1}{F_{\alpha,\beta,\mathrm{a},\mathrm{b}}(t)}\int_0^{t}(t-x)^s\,dF_{\alpha,\beta,\mathrm{a},\mathrm{b}}(X).$$

Then, the s^{th} moment of the reversed residual life of X becomes

$$A_s(0,t) = \frac{1}{F_{\alpha,\beta,\mathrm{a},\mathrm{b}}(t)}\sum_{k,v=0}^{\infty} C_{k,v}^{(\mathrm{a}k,s)}\,\mathrm{b}^s\gamma(s+1,\mathrm{b}t)|r > -1, \tag{12}$$

where $C_{k,v}^{(\mathrm{a}k,s)} = C_k\sum_{r=0}^{s}\binom{s}{r}(-1)^r t^{s-r}$.

3. Characterizing the new model

3.1 Based on two truncated moments

This subsection picks up the characterizations of ExEE distribution based on a relationship between two truncated moments. The first characterization applies a theorem of Glänzel (1987). Clearly, the result holds as well when the H is not a closed interval. This characterization is stable in the sense of weak convergence, see Glänzel (1990).

Proposition 3.1.1. Let the random variable $X: \Omega \to (0,\infty)$ be continuous, and let

$$\hbar(x)=\frac{\left\{1-\left[1-\left(1-e^{-\mathrm{b}x}\right)^{\mathrm{a}}\right]^{\alpha}+\left[1-\left(1-e^{-\mathrm{b}x}\right)^{\mathrm{a}}\right]^{\beta}\right\}^{2}}{\beta+(\alpha-\beta)[1-(1-e^{-\mathrm{b}x})^{\mathrm{a}}]^{\alpha}}$$

and $k(x)=\hbar(x)\left[1-\left(1-e^{-\mathrm{b}x}\right)^{\mathrm{a}}\right]$ for $x>0$. Then, the PDF of X is given in (5) if and only if the function η defined in Glänzel (1987) is

$$\eta(x)=\frac{\beta}{\beta+1}\left[1-\left(1-e^{-\mathrm{b}x}\right)^{\mathrm{a}}\right],\quad x>0.$$

Proof. If X has PDF (5), then

$$\left(1-F(x)\right)E[\hbar(X)\mid X\geq x]=\int_{x}^{\infty}\mathrm{ab}\,e^{-\mathrm{b}u}\left(1-e^{-\mathrm{b}u}\right)^{\mathrm{a}-1}\left[1-\left(1-e^{-\mathrm{b}u}\right)^{\mathrm{a}}\right]^{\beta-1}du=\frac{1}{\beta}\left[1-\left(1-e^{-\mathrm{b}x}\right)^{\mathrm{a}}\right]^{\beta},x>0,$$

and

$$\begin{aligned}\left(1-F(x)\right)E[k(X)\mid X\geq x]&=\int_{x}^{\infty}\mathrm{ab}\,e^{-\mathrm{b}u}\left(1-e^{-\mathrm{b}u}\right)^{\mathrm{a}-1}\left[1-\left(1-e^{-\mathrm{b}u}\right)^{\mathrm{a}}\right]^{\beta}du\\&=\frac{1}{\beta+1}\frac{1}{\beta}\left[1-\left(1-e^{-\mathrm{b}x}\right)^{\mathrm{a}}\right]^{\beta+1},x>0,\end{aligned}$$

and finally

$$\eta(x)\hbar(x)-k(x)=-\frac{1}{\beta+1}\hbar(x)\left[1-\left(1-e^{-\mathrm{b}x}\right)^{\mathrm{a}}\right]<0,\quad for\ x>0.$$

Conversely, if η has the above form, then

$$s'(x)=\frac{\eta'(x)\hbar(x)}{\eta(x)\hbar(x)-k(x)}=\frac{\mathrm{ab}\beta e^{-\mathrm{b}x}\left(1-e^{-\mathrm{b}x}\right)^{\mathrm{a}-1}}{1-(1-e^{-\mathrm{b}x})^{\mathrm{a}}},$$

and hence

$$s(x)=-\beta\,log\{\left[1-\left(1-e^{-\mathrm{b}x}\right)^{\mathrm{a}}\right]\},\quad x>0.$$

In view of Theorem of Glänzel (1987), X has PDF (5).

Corollary 3.1.1. If $X:\Omega\to(0,\infty)$ is a continuous random variable and $\hbar(x)$ is as in Proposition A.1.1. Then, X has PDF (5) if and only if there exist functions k and η defined in of Glänzel (1987) satisfying the following first order differential equation

$$\frac{\eta'(x)\hbar(x)}{\eta(x)\hbar(x)-k(x)}=\frac{\mathrm{ab}\beta e^{-\mathrm{b}x}\left(1-e^{-\mathrm{b}x}\right)^{\mathrm{a}-1}}{1-(1-e^{-\mathrm{b}x})^{\mathrm{a}}}.$$

Corollary 3.1.2. The general solution of the differential equation in Corollary A.1.1 is

$$\eta(x)=\left[1-\left(1-e^{-\mathrm{b}x}\right)^{\mathrm{a}}\right]^{-\beta}\left[\begin{array}{c}-\int\beta\,\mathrm{ab}e^{-\mathrm{b}x}\left(1-e^{-\mathrm{b}x}\right)^{\mathrm{a}-1}\times\\\left[1-\left(1-e^{-\mathrm{b}x}\right)^{\mathrm{a}}\right]^{\beta-1}\left(\hbar(x)\right)^{-1}k(x)+D\end{array}\right],$$

where D is a constant.

Proof. If X has PDF (5), then clearly the differential equation holds. Now, if the differential equation holds, then

$$\eta'(x)=\left(\frac{\mathrm{ab}\beta e^{-\mathrm{b}x}\left(1-e^{-\mathrm{b}x}\right)^{\mathrm{a}-1}}{1-(1-e^{-\mathrm{b}x})^{\mathrm{a}}}\right)\eta(x)-\left(\frac{\mathrm{ab}\beta e^{-\mathrm{b}x}\left(1-e^{-\mathrm{b}x}\right)^{\mathrm{a}-1}}{1-(1-e^{-\mathrm{b}x})^{\mathrm{a}}}\right)\left(\boldsymbol{q}_1(x)\right)^{-1}\boldsymbol{q}_2(x),$$

or

$$\eta'(x)-\left(\frac{\mathrm{ab}\beta e^{-\mathrm{b}x}\left(1-e^{-\mathrm{b}x}\right)^{\mathrm{a}-1}}{1-(1-e^{-\mathrm{b}x})^{\mathrm{a}}}\right)\eta(x)=-\left(\frac{\mathrm{ab}\beta e^{-\mathrm{b}x}\left(1-e^{-\mathrm{b}x}\right)^{\mathrm{a}-1}}{1-(1-e^{-\mathrm{b}x})^{\mathrm{a}}}\right)\left(\boldsymbol{q}_1(x)\right)^{-1}\boldsymbol{q}_2(x),$$

or

$$\begin{aligned}\left(1-\left(1-e^{-\mathrm{b}x}\right)^{\mathrm{a}}\right)^{\beta}\eta'(x)-\left(\mathrm{ab}\beta e^{-\mathrm{b}x}\left(1-e^{-\mathrm{b}x}\right)^{\mathrm{a}-1}\right)\left(1-\left(1-e^{-\mathrm{b}x}\right)^{\mathrm{a}}\right)^{\beta-1}\eta(x)\\=-\left(\mathrm{ab}\beta e^{-\mathrm{b}x}\left(1-e^{-\mathrm{b}x}\right)^{\mathrm{a}-1}\right)\left(1-\left(1-e^{-\mathrm{b}x}\right)^{\mathrm{a}}\right)^{\beta-1}\left(\boldsymbol{q}_1(x)\right)^{-1}\boldsymbol{q}_2(x),\end{aligned}$$

or

$$\frac{d}{dx}\left\{\left(1-\left(1-e^{-\mathrm{b}x}\right)^{\mathrm{a}}\right)^{\beta}\eta(x)\right\}=-\left(\mathrm{ab}\beta e^{-\mathrm{b}x}\left(1-e^{-\mathrm{b}x}\right)^{\mathrm{a}-1}\right)\left(1-\left(1-e^{-\mathrm{b}x}\right)^{\mathrm{a}}\right)^{\beta-1}\left(\boldsymbol{q}_1(x)\right)^{-1}\boldsymbol{q}_2(x),$$

from which we arrive at

$$\eta(x)=\left(1-\left(1-e^{-\mathrm{b}x}\right)^{\mathrm{a}}\right)^{-\beta}\left[-\int\left(\mathrm{ab}\beta e^{-\mathrm{b}x}\left(1-e^{-\mathrm{b}x}\right)^{\mathrm{a}-1}\right)\left(1-\left(1-e^{-\mathrm{b}x}\right)^{\mathrm{a}}\right)^{\beta-1}\left(\boldsymbol{q}_1(x)\right)^{-1}\boldsymbol{q}_2(x)dx+D\right].$$

A set of functions satisfying this differential equation is presented in Proposition A.1.1 with $D=0$. Clearly, there are other triplets $(\hbar,k,\eta)$ satisfying the conditions of Theorem of Glänzel (1987).

3.2 Characterization in terms of the hazard function

The hazard function, $\hbar_F$, of a twice differentiable distribution function, F, satisfies the following first order differential equation

$$\frac{f\,'(X)}{f\,(X)}=\frac{\hbar_F'(X)}{\hbar_F(X)}-\hbar_F(X).$$

It should be mentioned that for many univariate continuous distributions, the above equation is the only differential equation available in terms of the hazard function. In this subsection we present a characterization of the ExEE distribution in terms of the hazard function, which is not of the above trivial form.

Proposition 3.2.1. Let $X:\Omega\to(0,\infty)$ be a continuous random variable. The random variable X has pdf (5) if and only if its hazard function $\hbar_F(x)$ satisfies the following differential equation

$$\hbar_F'(x)-(\mathrm{a}-1)e^{-\mathrm{b}x}\left(1-e^{-\mathrm{b}x}\right)^{-1}\hbar_F(x)=\mathrm{ab}\left(1-e^{-\mathrm{b}x}\right)^{\mathrm{a}-1}\times\frac{d}{dx}\left\{\frac{e^{-\mathrm{b}x}\left(1-\left(1-e^{-\mathrm{b}x}\right)^{\beta-1}\right)\left[\beta+(\alpha-\beta)\left(1-\left(1-e^{-\mathrm{b}x}\right)^{\mathrm{a}}\right)^{\alpha}\right]}{(1-(1-e^{-\mathrm{b}x})^{\mathrm{a}})[(1-(1-e^{-\mathrm{b}x})^{\mathrm{a}})^{\alpha}+(1-(1-e^{-\mathrm{b}x})^{\mathrm{a}})^{\beta}]}\right\},$$

$x>0$, with the boundary condition $lim_{x\to0}\,\hbar_F(x)=0$ for $\mathrm{a}>1$.

Proof. Is straightforward.

3.3 Based on the conditional expectation of certain function of the random variable

In this subsection we employ a single function ϕ of X and characterize the distribution of X in terms of the truncated moment of $\phi(X)$.

Proposition 3.3.1. Let $X:\Omega\to(e,f)$ be a continuous random variable with CDF F. Let $\phi(x)$ be a differentiable function on (e,f) with $lim_{x\to e^+}\phi(x)=1$. Then for $\delta\neq1$, $E[\phi(X)\mid X\geq x]=\delta\phi(x)$, $x\in(e,f)$, if and only if

$$\phi(x)=\left(1-F(x)\right)^{\frac{1}{\delta}-1},\quad x\in(e,f)$$

Remark 3.3.1

For $(e,f)=(0,\infty)$, $\phi(x)=\frac{\left[1-\left(1-e^{-\mathrm{b}x}\right)^{\mathrm{a}}\right]}{\left\{1-\left[1-\left(1-e^{-\mathrm{b}x}\right)^{\mathrm{a}}\right]^{\alpha}+\left[1-\left(1-e^{-\mathrm{b}x}\right)^{\mathrm{a}}\right]^{\beta}\right\}^{1/\beta}}$ and $\delta=\frac{\beta}{\beta+1}$, Proposition 3.3.1. provides a characterization of the ExEE distribution.

4.Estimation methods

MLE method

Let $X_1,X_2,\ldots,X_n$ be a random sample (RS) from the ExEE distribution. The log-likelihood function for $\underline{\boldsymbol{\Psi}}$ where $\underline{\boldsymbol{\Psi}}=(\alpha,\beta,\mathrm{a},\mathrm{b})$ is given by $\ell(\underline{\boldsymbol{\Psi}})=\sum_{i=1}^{n}ln\left[f_{\alpha,\beta,\mathrm{a},\mathrm{b}}(X)\right]$ which can be maximized either using the statistical programs or by solving the nonlinear system obtained from $\ell(\underline{\boldsymbol{\Psi}})$ by differentiation. The score vector

$$U(\underline{\boldsymbol{\Psi}})=\left(\partial\ell(\underline{\boldsymbol{\Psi}})/\partial\alpha,\partial\ell(\underline{\boldsymbol{\Psi}})/\partial\beta,\partial\ell(\underline{\boldsymbol{\Psi}})/\partial\mathrm{a},\partial\ell(\underline{\boldsymbol{\Psi}})/\partial\mathrm{b}\right)^{\mathrm{T}}.$$

Setting

$$\partial\ell(\underline{\boldsymbol{\Psi}})/\partial\alpha=0,\partial\ell(\underline{\boldsymbol{\Psi}})/\partial\beta=0,\partial\ell(\underline{\boldsymbol{\Psi}})/\partial\mathrm{a}=0,\partial\ell(\underline{\boldsymbol{\Psi}})/\partial\mathrm{b}=0,$$

and solving them simultaneously yields the maximum likelihood estimates (MLETs) MLETs for the ExEE family parameters. The Newton-Raphson algorithms is employed for the numerically solving in such cases.

OLSE method

Let $F_{\alpha,\beta,\mathrm{a},\mathrm{b}}(x_i)$ denotes the CDF of ExEE model and let $x_1<x_2<\cdots<x_n$ be the n ordered RS. The OLSEs are obtained upon minimizing

$$OLSE(\underline{\boldsymbol{\Psi}}) = \sum_{i=1}^{n}\left[F_{\alpha,\beta,\mathrm{a},\mathrm{b}}(x_i) - c_{i,n}\right]^2,$$

where $c_{i,n} = \frac{i}{n+1}$ .The LSEs are obtained via solving the following non-linear equations

$$0 = \sum_{i=1}^{n}\left[F_{\alpha,\beta,\mathrm{a},\mathrm{b}}(x_i) - c_{i,n}\right]D_{(\alpha)}(x_i,\underline{\boldsymbol{\Psi}}), 0 = \sum_{i=1}^{n}\left[F_{\alpha,\beta,\mathrm{a},\mathrm{b}}(x_i) - c_{i,n}\right]D_{(\beta)}(x_i,\underline{\boldsymbol{\Psi}}),$$

$$0 = \sum_{i=1}^{n}\left[F_{\alpha,\beta,\mathrm{a},\mathrm{b}}(x_i) - c_{i,n}\right]D_{(\mathrm{a})}(x_i,\underline{\boldsymbol{\Psi}}), 0 = \sum_{i=1}^{n}\left[F_{\alpha,\beta,\mathrm{a},\mathrm{b}}(x_i) - c_{i,n}\right]D_{(\mathrm{b})}(x_i,\underline{\boldsymbol{\Psi}}),$$

where $D_{(\alpha)}(x_i,\underline{\boldsymbol{\Psi}})$, $D_{(\beta)}(x_i,\underline{\boldsymbol{\Psi}})$, $D_{(\mathrm{a})}(x_i,\underline{\boldsymbol{\Psi}})$ and $D_{(\mathrm{b})}(x_i,\underline{\boldsymbol{\Psi}})$ are the values of the first derivatives of the CDF of ExEE distribution with respect to α,β,a and b respectively.

ADE

The ADE are obtained by minimizing the function

$$ADE(\underline{\boldsymbol{\Psi}}) = -n - n^{-1}\sum_{i=1}^{n}(2i-1)\left\{log\, F_{\alpha,\beta,\mathrm{a},\mathrm{b}}\left(x_{i\ :\ n}\right) + log\left[1 - F_{(\gamma,\tau)}(x_{-i+1+n\ :\ n})\right]\right\}.$$

Then, the parameter estimates are obtained by solving the nonlinear equations

$$\frac{\partial}{\partial\alpha}\left[ADE(\underline{\boldsymbol{\Psi}})\right] = 0, \frac{\partial}{\partial\beta}\left[ADE(\underline{\boldsymbol{\Psi}})\right] = 0, \frac{\partial}{\partial\mathrm{a}}\left[ADE(\underline{\boldsymbol{\Psi}})\right] = 0 \text{ and } \frac{\partial}{\partial\mathrm{b}}\left[ADE(\underline{\boldsymbol{\Psi}})\right] = 0.$$

RTADE method

The RTADE are obtained by minimizing the function

$$RADE(\gamma,\tau) = \frac{n}{2} - 2\sum_{i=1}^{n}F_{\alpha,\beta,\mathrm{a},\mathrm{b}}(x_{i\ :\ n}) - \frac{1}{n}\sum_{i=1}^{n}(2i-1)\left\{log\left[1 - F_{\alpha,\beta,\mathrm{a},\mathrm{b}}(x_{-i+1+n\ :\ n})\right]\right\}.$$

LAD 2 method

The LAD2 estimates (LADSOE) are obtained by minimizing

$$\mathrm{LAD2}(\underline{V}) = 2\sum_{i=1}^{n}log\left[F_{\alpha,\beta,\mathrm{a},\mathrm{b}}(x_{i\ :\ n})\right] + \frac{1}{n}\sum_{i=1}^{n}\frac{2i-1}{F_{\alpha,\beta,\mathrm{a},\mathrm{b}}(x_{i\ :\ n})}.$$

Then, the parameter estimates can be obtained by solving the nonlinear equations

$$\partial[\mathrm{LAD}]2(\underline{V})]/\partial\alpha = 0, \partial[\mathrm{LAD}]2(\underline{V})]/\partial\beta = 0, \partial[\mathrm{LAD}]2(\underline{V})]/\partial\mathrm{a} = 0 \text{ and } \partial[\mathrm{LAD}]2(\underline{V})]/\mathrm{b} = 0.$$

5. Assessing methods

The choice of estimation method plays a crucial role in accurately inferring parameters from data, particularly in the context of complex probability distributions. This Section presents a comprehensive simulation study aimed at evaluating the performance and behavior of several estimators applied to a specific distribution, utilizing various combinations of parameter values and sample sizes. The estimators under investigation include MLE, OLSE, ADE, RTADE, and LAD2 methods. Each of these methods holds unique characteristics and assumptions, making their comparative analysis essential for selecting the most effective approach in practical applications. The simulation study examines three distinct sets of parameter combinations for the target distribution:

(1): $\alpha_0 = 2$, $\beta_0 = 2$, $\mathrm{a}_0 = 0.9$ and $\mathrm{b}_0 = 0.5$ (see Table 1);

(2): $\alpha_0 = 1.5$, $\beta_0 = 1.2$, $\mathrm{a}_0 = 1.2$ and $\mathrm{b}_0 = 0.9$ (see Table 2);

(3): $\alpha_0 = 2.5$, $\beta_0 = 2$, $\mathrm{a}_0 = 2.5$ and $\mathrm{b}_0 = 2$ (see Table 3).

These combinations encompass a range of scenarios to explore how the estimators respond to varying degrees of parameter complexity and distribution characteristics. Furthermore, the impact of sample size on estimator performance is investigated using four different sample sizes: $20,50,100,$ and 300 . This aspect of the study is crucial as it sheds light on the robustness and efficiency of the estimators under different data availability scenarios, providing insights into their scalability and reliability in practical settings. The evaluation criteria employed in this simulation study include measures of bias (BIAS[·]), root mean squared error (RMSE[·]), mean absolute differences (D_{abs}), and maximum absolute differences (D_{max}). These criteria collectively assess the accuracy, precision, and robustness of the estimators across the varied parameter settings and sample sizes, enabling a comprehensive comparison and selection of optimal estimation methods for specific modeling contexts. The outcomes of this simulation study are expected to

contribute significantly to the understanding of estimator behavior in complex statistical modeling, offering practical guidance for researchers and practitioners in selecting appropriate methods for parameter inference based on distributional assumptions and data characteristics.

The subsequent sections detail the methodology, results, and implications derived from this comprehensive investigation. Based on Table 1:

1) For $n = 20$: RTADE appears to be the most effective method with the lowest bias, RMSE, D_{abs}, and D_{max} values, indicating accurate and precise parameter estimation. ADE also shows promising performance with reduced bias and RMSE compared to MLE and OLSE. MLE and OLSE exhibit moderate performance with notable bias and RMSE, highlighting room for improvement. LAD2 demonstrates less desirable performance with substantial bias and high RMSE, suggesting limitations in accurate parameter estimation.
2) For $n = 50$: MLE stands out as the most effective method with very low bias, low RMSE, and minimal discrepancies (D_{abs}, D_{max}) between estimated and true parameter values. OLSE, ADE, and RTADE demonstrate consistent and reliable performance with moderate bias and RMSE, as well as reasonable agreement (Dabs, Dmax) between estimated and true values. LAD2 exhibits relatively poorer performance with notable bias, higher RMSE, and larger discrepancies (D_{abs}, D_{max}) in parameter estimation compared to other methods.
3) For $n = 100$: MLE demonstrates excellent performance with very low bias, low RMSE, and minimal discrepancies (D_{abs}, D_{max}) between estimated and true parameter values. OLSE, ADE, and RTADE exhibit consistent and reliable performance with low to moderate bias, as well as moderate RMSE values and good agreement (D_{abs}, D_{max}) between estimated and true values. LAD2 shows reasonable performance with low to moderate bias, moderate RMSE values, and acceptable agreement (Dabs, Dmax) between estimated and true values.
4) For $n = 300$: MLE demonstrates outstanding performance with extremely low bias, low RMSE, and minimal discrepancies (D_{abs}, D_{max}) between estimated and true parameter values. OLSE, ADE, RTADE, and LAD 2 exhibit consistent and reliable performance with low bias, moderate RMSE values, and good agreement (Dabs, Dmax) between estimated and true values. RTADE stands out with particularly low bias and exceptionally small Dabs and Dmax values, indicating highly accurate parameter estimation.

Based on Table 2:

- For $n = 20$: MLE and LAD 2 demonstrate higher bias and RMSE values, suggesting less accurate and less precise estimation compared to other methods. OLSE, ADE, and RTADE exhibit more moderate bias and RMSE values, with varying degrees of accuracy and precision in parameter estimation. RTADE shows relatively improved performance with lower D_{abs} and D_{max} values compared to other methods, indicating better agreement between estimated and true parameter values.
- For $n = 50$: MLE exhibits moderate bias and RMSE values, suggesting reasonably accurate but not highly precise estimation. OLSE, ADE, RTADE, and LAD 2 demonstrate varying degrees of bias and RMSE values, with generally acceptable levels of accuracy and precision in parameter estimation. LAD 2 shows slightly higher bias compared to other methods, particularly for β, with comparable levels of RMSE and agreement (D_{abs}, D_{max}) between estimated and true values.
- For $n = 100$: MLE demonstrates excellent performance with low bias, low RMSE, and minimal discrepancies (D_{abs}, D_{max}) between estimated and true parameter values. OLSE, ADE, RTADE, and LAD2 exhibit consistent and reliable performance with low bias and RMSE values, as well as good agreement (D_{abs}, D_{max}) between estimated and true values. RTADE stands out with very low RMSE values, indicating high precision in parameter estimation.
- MLE, OLSE, ADE, RTADE, and LAD 2 all demonstrate outstanding performance with very low bias, very low RMSE, and exceptionally minimal discrepancies (D_{abs}, D_{max}) between estimated and true parameter values. These findings highlight the effectiveness of the evaluated estimation methods in accurately estimating parameters from data with a relatively large sample size of $n = 300$. The larger sample size significantly contributes to improved estimation accuracy and precision, emphasizing the importance of sufficient data for reliable statistical inference.

Based on Table 3:

1) For $n = 20$: MLE and LAD2 demonstrate higher bias and RMSE values, suggesting less accurate and less precise estimation compared to other methods. OLSE, ADE, and RTADE exhibit varying degrees of bias and RMSE values, with generally acceptable levels of accuracy and precision in parameter estimation. These findings highlight the challenges of parameter estimation with smaller sample sizes ($n = 20$) and underscore the

importance of selecting appropriate estimation methods based on bias, RMSE, D_{abs}, and D_{max} metrics to ensure reliable and accurate parameter inference from data. Larger sample sizes typically lead to improved estimation performance, reducing biases and enhancing precision in parameter estimation.

2) For $n = 50$: MLE and OLSE demonstrate moderate bias and RMSE values, suggesting reasonably accurate but less precise estimation compared to other methods. ADE, RTADE, and LAD 2 exhibit varying degrees of bias and RMSE values, with generally acceptable levels of accuracy and precision in parameter estimation. These findings highlight the performance characteristics of different estimation methods under sample size $n = 50$, providing insights into their relative accuracy, precision, and reliability in parameter estimation tasks. Adjustments in method selection may be considered based on specific requirements for bias, RMSE, and agreement metrics in practical applications.
3) For $n = 100$: MLE demonstrates relatively low bias and RMSE values, suggesting accurate and precise estimation compared to other methods. OLSE, ADE, RTADE, and LAD 2 exhibit varying degrees of bias and RMSE values, with generally acceptable levels of accuracy and precision in parameter estimation.
4) For $n = 300$: MLE, OLSE, ADE, RTADE, and LAD 2 demonstrate low bias and RMSE values, indicating accurate and precise estimation of parameters. These findings provide insights into the performance characteristics of different estimation methods under a larger sample size ($n = 300$), highlighting their relative accuracy, precision, and reliability in parameter estimation tasks. Overall, the estimation methods perform well with reduced biases and excellent precision, reflecting robustness in handling larger datasets for parameter inference. Adjustments in method selection may be considered based on specific requirements for bias, RMSE, and agreement metrics in practical applications.
5)

Based on the analysis of simulation results across Table 1, Table 2, and Table 3 for different sample sizes ($n = 20, n = 50, n = 100$ and $n = 300$) and various estimation methods (MLE, OLSE, ADE, RTADE, LAD2), several observations can be made:

- Sample size $n = 20$: MLE and OLSE exhibit moderate to high bias and RMSE values, indicating less accurate and less precise estimation, especially noticeable in smaller sample sizes. ADE, RTADE, and LAD2 generally show varying degrees of bias and RMSE, with relatively acceptable levels of accuracy and precision in parameter estimation. RTADE stands out as a promising method with lower bias, RMSE, and better agreement (D_{abs}, D_{max}) between estimated and true parameter values compared to others.
- Sample size $n = 50$: MLE demonstrates reasonable accuracy but less precision with moderate bias and RMSE. OLSE, ADE, RTADE, and LAD2 exhibit varying degrees of bias and RMSE, generally showing acceptable levels of accuracy and precision in parameter estimation. RTADE again shows relatively improved performance with lower D_{abs} and D_{max} values compared to other methods.
- Sample size $n = 100$: MLE consistently shows excellent performance with low bias, low RMSE, and minimal discrepancies (D_{abs}, D_{max}) between estimated and true parameter values. OLSE, ADE, RTADE, and LAD 2 demonstrate consistent and reliable performance with varying degrees of bias and RMSE, maintaining good accuracy and precision in parameter estimation across different sample sizes.
- Sample size $n = 300$: MLE, OLSE, ADE, RTADE, and LAD2 consistently demonstrate low bias and RMSE values, indicating accurate and precise parameter estimation, especially with larger sample sizes. RTADE particularly stands out with very low bias and exceptionally small D_{abs} and D_{max} values, suggesting highly accurate parameter estimation.
- The performance of estimation methods varies across different sample sizes, with larger sample sizes generally resulting in improved accuracy and precision. RTADE consistently shows promising performance across sample sizes, indicating its robustness in accurate parameter estimation. MLE and OLSE tend to exhibit slightly higher bias and RMSE in smaller sample sizes, suggesting the need for caution and potential adjustments in method selection based on sample size and specific requirements for bias and precision. LAD 2 generally exhibits relatively poorer performance compared to other methods, particularly in smaller sample sizes.
- Finally, the simulation results suggest that MLE and RTADE are among the more robust methods in terms of low bias, consistency, and efficiency across different sample sizes. As sample size increases, bias tends to decrease for most methods, reflecting improvement towards unbiased parameter estimation. The efficiency of estimation methods, reflected in lower RMSE values, highlights the importance of sample size in achieving accurate and precise parameter estimation.

Table 1: Simulation results for parameters α=2,β=2,a=0.9 and b=0.5.

	$BIAS_\alpha$	$BIAS_\beta$	$BIAS_a$	$BIAS_b$	$RMSE_\alpha$	$RMSE_\beta$	$RMSE_a$	$RMSE_b$	D_{abs}	D_{max}
n=20										
MLE	0.31070	0.19573	0.02171	0.03271	1.70912	0.67737	0.15298	0.13755	0.0348	0.0514

OLSE	0.42116	0.15515	0.01011	0.02349	1.58471	0.93397	0.16365	0.15066	0.0375	0.0541
ADE	0.39419	0.13042	0.00833	0.02210	1.52904	0.75764	0.15717	0.13962	0.0348	0.0502
RTADE	0.30518	0.0882	0.03045	0.01261	1.4406	0.71878	0.18673	0.13619	0.0152	0.0227
LAD_2	0.43011	0.39332	0.00320	0.04499	1.57832	2.22151	0.15450	0.20613	0.0648	0.0950
n=50										
MLE	0.06467	0.06343	0.01531	0.00944	0.71815	0.37626	0.09903	0.08042	0.0062	0.0111
OLSE	0.13738	0.05582	0.00623	0.00823	0.76998	0.52998	0.10361	0.09058	0.0124	0.0181
ADE	0.12329	0.04841	0.00578	0.00756	0.74861	0.44779	0.09902	0.08484	0.0111	0.0161
RTADE	0.14748	0.04027	0.00912	0.00665	0.82840	0.41420	0.11497	0.08151	0.0099	0.0148
LAD_2	0.12709	0.12100	0.00384	0.01405	0.73442	0.65531	0.09628	0.10206	0.0198	0.0295
n=100										
MLE	0.04503	0.03741	0.00429	0.00634	0.48470	0.25120	0.06700	0.05450	0.0062	0.0095
OLSE	0.05126	0.01919	0.00493	0.00254	0.50259	0.35453	0.07168	0.06168	0.0033	0.0049
ADE	0.04329	0.01548	0.00477	0.00204	0.48906	0.29714	0.06840	0.05735	0.0025	0.0038
RTADE	0.05714	0.01241	0.00683	0.00174	0.57759	0.27588	0.07917	0.05585	0.0020	0.0032
LAD_2	0.04345	0.04811	0.00390	0.00467	0.47307	0.42471	0.06645	0.06797	0.0062	0.0098
n=300										
MLE	0.02649	0.00416	0.00116	0.00105	0.28363	0.13648	0.03922	0.03010	0.0017	0.0026
OLSE	0.02875	0.00998	0.00035	0.00179	0.29629	0.19964	0.04225	0.03600	0.0029	0.0043
ADE	0.02084	0.00307	0.00125	0.00068	0.29048	0.16959	0.04057	0.03356	0.0012	0.0018
RTADE	0.00184	-0.00362	0.00445	-0.00105	0.30907	0.15619	0.04435	0.03156	0.0024	0.0033
LAD_2	0.02864	0.02211	-0.00008	0.00314	0.28777	0.23720	0.04047	0.04069	0.0046	0.0067

Table 2: Simulation results for parameters α=1.5,β=1.2,a=1.2 and b=0.9.

	$BIAS_\alpha$	$BIAS_\beta$	$BIAS_a$	$BIAS_b$	$RMSE_\alpha$	$RMSE_\beta$	$RMSE_a$	$RMSE_b$	D_{abs}	D_{max}
n=20										
MLE	0.26386	0.15189	0.04037	0.06484	1.63323	0.46571	0.26539	0.24308	0.0409	0.0603
OLSE	0.32345	0.10246	0.03697	0.02833	1.21779	0.67180	0.30541	0.24693	0.0300	0.0436
ADE	0.25012	0.06457	0.04088	0.02106	1.10613	0.49319	0.28654	0.23102	0.0192	0.0285
RTADE	0.20744	0.05567	0.08858	0.01354	1.13441	0.46418	0.38683	0.22141	0.0053	0.0085
LAD_2	0.33199	0.27484	0.01959	0.05715	1.22925	1.16141	0.26632	0.29016	0.0587	0.0864
n=50										
MLE	0.07257	0.04010	0.02386	0.01467	0.56363	0.23337	0.15814	0.12964	0.0079	0.0128
OLSE	0.08384	0.02191	0.02110	0.00463	0.57740	0.33828	0.17853	0.14185	0.0045	0.0071
ADE	0.08224	0.0177	0.01754	0.00541	0.58432	0.26105	0.16793	0.13177	0.0050	0.0077
RTADE	0.08780	0.02663	0.02817	0.00751	0.64145	0.25746	0.20531	0.13073	0.0046	0.0074
LAD_2	0.08090	0.06495	0.01434	0.01296	0.55034	0.42233	0.15971	0.15609	0.0127	0.0195
n=100										
MLE	0.03445	0.02831	0.00944	0.01207	0.35571	0.14864	0.10707	0.08419	0.0067	0.0104
OLSE	0.04158	0.01044	0.01227	0.00201	0.41196	0.22952	0.12872	0.10217	0.0017	0.0028
ADE	0.03201	0.01010	0.01228	0.00173	0.39443	0.19193	0.12197	0.09649	0.0011	0.0019
RTADE	0.05285	0.01867	0.00915	0.00666	0.00666	0.17863	0.13697	0.09190	0.00544	0.0080
LAD_2	0.04195	0.03225	0.00823	0.00654	0.39661	0.28191	0.11524	0.11347	0.00632	0.0097
n=300										
MLE	0.00653	0.00621	0.00433	0.00187	0.20548	0.08694	0.06143	0.05046	0.0007	0.0015
OLSE	0.01015	0.00476	0.00439	0.00066	0.21755	0.12669	0.07019	0.05676	0.0004	0.0008
ADE	0.00543	0.00330	0.00517	-0.00003	0.21569	0.10754	0.0675	0.05418	0.0005	0.0009
RTADE	0.01359	0.00361	0.00484	0.00098	0.24433	0.09780	0.08004	0.05222	0.0005	0.0009
LAD_2	0.00525	0.00990	0.00473	0.00069	0.20504	0.14776	0.06302	0.06137	0.0008	0.0017

Table 3: Simulation results for parameters α=2.5,β=2,a=2.5 and b=2.

	$BIAS_\alpha$	$BIAS_\beta$	$BIAS_a$	$BIAS_b$	$RMSE_\alpha$	$RMSE_\beta$	$RMSE_a$	$RMSE_b$	D_{abs}	D_{max}
n=20										
MLE	0.42587	0.14441	0.07765	0.02292	2.29964	0.66691	0.44144	0.28927	0.0189	0.0278
OLSE	0.38565	0.10003	0.08056	0.00292	1.79808	0.97756	0.49433	0.31452	0.0103	0.0158
ADE	0.46928	0.13621	0.06163	0.02038	2.04073	0.87150	0.48770	0.32849	0.0216	0.0316
RTADE	0.40247	0.09285	0.09116	0.01168	1.96309	0.71049	0.53977	0.30077	0.0109	0.0167
LAD_2	0.42003	0.33504	0.05369	0.02672	2.10483	1.54605	0.44997	0.34726	0.0341	0.0507
n=50										
MLE	0.14054	0.07544	0.02526	0.01775	1.00515	0.37419	0.27158	0.18803	0.0106	0.015
OLSE	0.15006	0.04358	0.03411	0.00079	1.04691	0.58105	0.30245	0.20663	0.0042	0.0064
ADE	0.12951	0.04835	0.03093	0.00461	0.99147	0.47837	0.29013	0.19743	0.0049	0.0074
RTADE	0.21517	0.06175	0.01654	0.01584	1.08688	0.44362	0.31913	0.19445	0.0134	0.01951
LAD_2	0.14688	0.12443	0.02414	0.00982	1.00728	0.82034	0.27833	0.22268	0.0124	0.0189
n=100										
MLE	0.02993	0.04212	0.02171	0.00660	0.60382	0.26390	0.19029	0.13132	0.0025	0.0049
OLSE	0.12641	0.05077	-0.00383	0.01345	0.66911	0.37687	0.19884	0.13908	0.0117	0.0166
ADE	0.12613	0.03379	-0.00691	0.01233	0.65514	0.31139	0.18658	0.13265	0.0108	0.0156
RTADE	0.07613	0.02399	0.01639	0.00391	0.71721	0.28583	0.22498	0.13214	0.0032	0.0047

LAD_2 n=300	0.12024	0.09178	-0.00772	0.01882	0.62893	0.45886	0.18322	0.14787	0.1478	0.0223
MLE	0.02898	0.00768	0.00321	0.00230	0.35389	0.13990	0.10785	0.07311	0.0017	0.0025
OLSE	0.02579	0.00799	0.00451	0.00080	0.38112	0.21088	0.11827	0.08171	0.0011	0.0016
ADE	0.02140	0.00829	0.00452	0.00095	0.37222	0.17826	0.11360	0.07846	0.0009	0.0015
RTADE	0.01963	0.00363	0.00801	-0.00041	0.41769	0.16294	0.12970	0.07721	0.0001	0.0003
LAD_2	0.02522	0.01990	0.00285	0.00235	0.36015	0.25257	0.11045	0.08744	0.0024	0.0035

6. The empirical risk analysis under different estimation methods

The robust performance of key risk indicators (KRIs) across different sample sizes and estimation methods underscores the reliability and effectiveness of these methods in risk analysis. The scalability of these methods is evident as sample sizes increase ($n = 20,50,100,300$). Performance metrics like bias and RMSE often improve with larger datasets, reflecting the ability of these methods to leverage more data for more accurate risk assessments. In this Section, a comprehensive robust performance of KRIs across sizes and methods are presented. For this main aim, the simulation study examines three distinct sets of parameter combinations for the target distribution: (1): $\alpha_0 = 2$, $\beta_0 = 2$, $\mathrm{a}_0 = 0.9$ and $\mathrm{b}_0 = 0.5$ (see Table 4, Table 5, Table 6 and Table 7); (2): $\alpha_0 = 1.5$, $\beta_0 = 1.2$, $\mathrm{a}_0 = 1.2$ and $\mathrm{b}_0 = 0.9$ (see Table 8, Table 9, Table 10, Table 11); and (3): $\alpha_0 = 2.5$, $\beta_0 = 2$, $\mathrm{a}_0 = 2.5$ and $\mathrm{b}_0 = 2$ (see Table 12, Table 13, Table 14, Table 15). Based on Table 4, Table 8 and Table 12: The estimation methods (MLE, OLSE, ADE, RTADE, LAD2) perform comparably in estimating key risk indicators under artificial data for a sample size of $n = 20$ and various quantiles (70%, 80%, 90%). They exhibit consistent behavior in reflecting increasing risk exposure at higher quantile levels, providing reliable estimates that align with the specified confidence levels. The results suggest that these methods are effective in estimating risk measures based on the provided artificial data and are suitable for capturing risk exposure across different levels of confidence. Based on Table 5, Table 9 and Table 13: The estimation methods (MLE, OLSE, ADE, RTADE, LAD2) perform comparably in estimating key risk indicators under artificial data for a sample size of $n = 50$ and various quantiles (70%, 80%, 90%). They exhibit consistent behavior in reflecting increasing risk exposure at higher quantile levels, providing reliable estimates that align with the specified confidence levels. The results suggest that these methods are effective in estimating risk measures based on the provided artificial data and are suitable for capturing risk exposure across different levels of confidence. Based on Table 6, Table 10 and Table 14, the estimation methods (MLE, OLSE, ADE, RTADE, LAD2) perform comparably in estimating key risk indicators under artificial data for a sample size of n=100n=100 and various quantiles (70%, 80%, 90%). They exhibit consistent behavior in reflecting increasing risk exposure at higher quantile levels, providing reliable estimates that align with the specified confidence levels. The results suggest that these methods are effective in estimating risk measures based on the provided artificial data and are suitable for capturing risk exposure across different levels of confidence. Based on Table 7, Table 11 and Table 15: The estimation methods (MLE, OLSE, ADE, RTADE, LAD2) perform consistently and reliably in estimating key risk indicators under artificial data for a larger sample size of $n = 300$ and various quantiles (70%, 80%, 90%). They exhibit stable behavior in reflecting increasing risk exposure at higher quantile levels, providing accurate and dependable estimates that align with the specified confidence levels. These results suggest that these methods are effective in estimating risk measures based on the provided artificial data and are suitable for capturing risk exposure across different levels of confidence, especially with the larger sample size.

Based on the comprehensive analysis of the results presented in Tables 4-15, which showcase KRIs under artificial data for varying sample sizes ($n = 20,50,100,300$) and different quantiles (70%, 80%, 90%), several insightful observations can be made regarding the performance of different estimation methods (MLE, OLSE, ADE, RTADE, LAD2) in analyzing and evaluating risks. Also, we can highlight the following results:

1) For the MLE: Consistently performs exceptionally well across all sample sizes and quantiles, with minimal bias and RMSE values, making it a strong choice for risk analysis.
2) For the RTADE: Particularly effective at larger sample sizes ($n = 300$), showing low bias and excellent precision, making it suitable for accurate risk assessment.
3) For the OLSE, ADE, LAD2 : Display reliable performance across different scenarios, providing good alternatives based on specific requirements and constraints.
4) For the large sample sizes ($n = 100,300$): the MLE emerges as the optimal method, offering exceptional accuracy and precision in risk estimation.
5) For the moderate sample sizes ($n = 50$): the MLE, OLSE, ADE, RTADE, and LAD 2 demonstrate competitive performance, providing robust options for risk analysis.
6) For the smaller sample sizes ($n = 20$): Despite challenges, RTADE shows promise in minimizing bias and RMSE, making it suitable for scenarios with limited data.

7) It is recommended to choose MLE for large sample sizes ($n = 100,300$) to ensure precise and reliable risk assessments.
8) We may consider RTADE for its consistent performance across different sample sizes, especially in scenarios with limited data.

Table 4: KRIs under artificial data for n=20|α_o=2, β_o=2, a_o=0.9 and b_o=0.5.

Method	α	β	a	b	VaRq(X)	TVaRq(X)	TVq(X)	TMVq(X)	MELq(X)
MLE	2.311	2.195	0.921	0.532					
70%					0.91995	1.75833	0.71529	2.11597	0.83838
80%					1.25587	2.0994	0.71928	2.45904	0.84353
90%					1.83782	2.68587	0.7231	3.04742	0.84804
OLSE	2.421	2.155	0.910	0.523					
70%					0.92100	1.79318	0.77445	2.18041	0.87218
80%					1.26972	2.14827	0.77839	2.53747	0.87855
90%					1.87630	2.75897	0.78093	3.14944	0.88267
ADE	2.394	2.130	0.908	0.522					
70%					0.93253	1.81703	0.79668	2.21536	0.88450
80%					1.28610	2.17714	0.80080	2.57754	0.89104
90%					1.90126	2.79655	0.80346	3.19829	0.89529
RTADE	2.305	2.088	0.930	0.512					
70%					1.00433	1.92909	0.86612	2.36215	0.92475
80%					1.37541	2.30519	0.86912	2.73975	0.92978
90%					2.01822	2.95094	0.87064	3.38626	0.93272
LAD_2	2.430	2.393	0.90	0.545					
70%					0.80889	1.55059	0.56421	1.83269	0.74170
80%					1.10502	1.85258	0.56908	2.13712	0.74756
90%					1.61928	2.37313	0.57471	2.66048	0.75385

Table 5: KRIs under artificial data for n=50|α_o=2, β_o=2, a_o=0.9 and b_o=0.5.

Method	α	β	a	b	VaRq(X)	TVaRq(X)	TVq(X)	TMVq(X)	MELq(X)
MLE	2.064	2.063	0.915	0.509					
70%					1.03513	1.96301	0.87803	2.40202	0.92788
80%					1.40694	2.34045	0.88396	2.78242	0.93351
90%					2.05015	2.98983	0.89085	3.43526	0.93968
OLSE	2.137	2.055	0.906	0.508					
70%					1.01703	1.95153	0.89170	2.39738	0.93450
80%					1.39080	2.33188	0.89777	2.78077	0.94108
90%					2.03930	2.98660	0.90402	3.43861	0.94730
ADE	2.123	2.048	0.905	0.507					
70%					1.02267	1.96149	0.90006	2.41152	0.93881
80%					1.39817	2.34359	0.90627	2.79672	0.94542
90%					2.04961	3.00135	0.91271	3.45771	0.95174
RTADE	2.147	2.040	0.909	0.506					
70%					1.02836	1.97526	0.91434	2.43243	0.94690
80%					1.40724	2.36062	0.92007	2.82066	0.95338
90%					2.06458	3.02371	0.92561	3.48652	0.95913
LAD_2	2.127	2.121	0.903	0.514					
70%					0.98071	1.87129	0.81162	2.27710	0.89057
80%					1.33682	2.23375	0.81805	2.64278	0.89693
90%					1.95419	2.85808	0.82553	3.27085	0.90389

Table 6: KRIs under artificial data for n=100α_o=2, β_o=2, a_o=0.9 and b_o=0.5.

Method	α	β	a	b	VaRq(X)	TVaRq(X)	TVq(X)	TMVq(X)	MELq(X)
MLE	2.045	2.037	0.904	0.506					
70%					1.03968	1.98250	0.90882	2.43690	0.94282
80%					1.41685	2.36618	0.91571	2.82403	0.94933
90%					2.07049	3.02687	0.92364	3.48869	0.95638
OLSE	2.051	2.019	0.904	0.502					
70%					1.05446	2.01464	0.94199	2.48564	0.96019

80%					1.43859	2.40540	0.94882	2.87981	0.96681
90%					2.10450	3.07815	0.95638	3.55634	0.97365
ADE	2.043	2.015	0.904	0.502					
70%					1.05804	2.02075	0.94702	2.49426	0.96271
80%					1.44319	2.41254	0.95391	2.88949	0.96935
90%					2.11082	3.08706	0.96160	3.56786	0.97624
RTADE	2.057	2.012	0.906	0.501					
70%					1.06042	2.02669	0.95327	2.50332	0.96626
80%					1.44709	2.41990	0.95988	2.89984	0.97281
90%					2.11733	3.09672	0.96705	3.58024	0.97939
LAD_2	2.043	2.048	0.903	0.504					
70%					1.03877	1.97892	0.90397	2.43090	0.94014
80%					1.41486	2.36151	0.91098	2.81700	0.94665
90%					2.06654	3.02038	0.91921	3.47998	0.95384

Table 7: KRIs under artificial data for n=300α_o=2, β_o=2, a_o=0.9 and b_o=0.5.

Method	α	β	a	b	VaRq(X)	TVaRq(X)	TVq(X)	TMVq(X)	MELq(X)
MLE	2.026	2.004	0.901	0.501					
70%					1.06246	2.03135	0.96005	2.51138	0.96889
80%					1.4499	2.42570	0.96735	2.90937	0.97579
90%					2.12177	3.10482	0.97556	3.59260	0.98305
OLSE	2.028	2.009	0.900	0.501					
70%					1.05709	2.02121	0.95092	2.49667	0.96412
80%					1.44257	2.41362	0.95827	2.89276	0.97106
90%					2.11109	3.08950	0.96659	3.57279	0.97840
ADE	2.020	2.003	0.901	0.500					
70%					1.06473	2.03468	0.96217	2.51576	0.96994
80%					1.45261	2.42944	0.96951	2.91420	0.97683
90%					2.12517	3.10930	0.97783	3.59821	0.98413
RTADE	2.001	1.996	0.904	0.498					
70%					1.07880	2.05590	0.97570	2.54374	0.97710
80%					1.46978	2.45350	0.98296	2.94498	0.98372
90%					2.14718	3.13808	0.99130	3.63373	0.99090
LAD_2	2.028	2.022	0.899	0.503					
70%					1.04894	2.00377	0.93306	2.47030	0.95484
80%					1.43069	2.39241	0.94045	2.86263	0.96172
90%					2.09266	3.06185	0.94896	3.53633	0.96919

Table 8: KRIs under artificial data for n=20|α_o=1.5, β_o=1.2, a_o=1.2.

Method	α	β	a	b	VaRq(X)	TVaRq(X)	TVq(X)	TMVq(X)	MELq(X)
MLE	1.763	1.351	1.240	0.964					
70%					1.02409	1.83889	0.63647	2.15712	0.81480
80%					1.36096	2.16767	0.62571	2.48052	0.80671
90%					1.92913	2.72185	0.61090	3.0273	0.79272
OLSE	1.823	1.302	1.236	0.928					
70%					1.07854	1.96367	0.74783	2.33758	0.88513
80%					1.44489	2.32079	0.73358	2.68758	0.87591
90%					2.06324	2.92176	0.71367	3.27860	0.85852
ADE	1.75012	1.26457	1.240	0.921					
70%					1.12187	2.03847	0.80323	2.44009	0.9166
80%					1.50100	2.40834	0.78848	2.80259	0.90735
90%					2.14111	3.03112	0.76786	3.41505	0.89001
RTADE	1.707	1.255	1.288	0.913					
70%					1.17637	2.10864	0.82896	2.52312	0.93227
80%					1.56275	2.48460	0.81324	2.89121	0.92184
90%					2.21332	3.11712	0.79181	3.51303	0.90380
LAD_2	1.832	1.474	1.219	0.957					
70%					0.95424	1.70382	0.54028	1.97396	0.74958
80%					1.26388	2.00632	0.53193	2.27229	0.74244

90%					1.78599	2.51677	0.52054	2.77704	0.73079

Table 9: KRIs under artificial data for n=50|α_0=1.5, β_0=1.2, a_0=1.2.

Method	α	β	a	b	VaRq(X)	TVaRq(X)	TVq(X)	TMVq(X)	MELq(X)
MLE	1.572	1.240	1.223	0.914					
70%					1.16296	2.09151	0.83189	2.50745	0.92855
80%					1.54568	2.46649	0.81995	2.87646	0.92081
90%					2.19268	3.09992	0.80334	3.50158	0.90723
OLSE	1.583	1.221	1.221	0.904					
70%					1.18286	2.13751	0.87847	2.57675	0.95466
80%					1.57636	2.52305	0.86540	2.95575	0.94669
90%					2.24195	3.17408	0.84701	3.59759	0.93213
ADE	1.582	1.218	1.217	0.905					
70%					1.18216	2.13913	0.88295	2.58060	0.95697
80%					1.57653	2.52563	0.86985	2.96055	0.94909
90%					2.24380	3.17833	0.85138	3.60403	0.93454
RTADE	1.588	1.227	1.228	0.907					
70%					1.18056	2.12911	0.86673	2.56248	0.94855
80%					1.57172	2.51213	0.85365	2.93896	0.94042
90%					2.23300	3.15878	0.83537	3.57647	0.92578
LAD_2	1.580	1.264	1.214	0.912					
70%					1.14207	2.05235	0.80052	2.45261	0.91028
80%					1.51707	2.41999	0.78950	2.81474	0.90292
90%					2.15113	3.04131	0.77418	3.42840	0.89018

Table 10: KRIs under artificial data for n=100|α_0=1.5, β_0=1.2, a_0=1.2.

Method	α	β	a	b	VaRq(X)	TVaRq(X)	TVq(X)	TMVq(X)	MELq(X)
MLE	1.534	1.228	1.209	0.912					
70%					1.17039	2.10717	0.84894	2.53165	0.93679
80%					1.55601	2.48560	0.83765	2.90442	0.92958
90%					2.20853	3.12543	0.82186	3.53636	0.91689
OLSE	1.541	1.210	1.212	0.902					
70%					1.19530	2.15854	0.89646	2.60676	0.96324
80%					1.59193	2.54763	0.88400	2.98963	0.95570
90%					2.26321	3.20522	0.86646	3.63845	0.94201
ADE	1.532	1.210	1.212	0.901					
70%					1.19781	2.16089	0.89656	2.60917	0.96308
80%					1.59433	2.54992	0.88429	2.99207	0.95560
90%					2.26539	3.20752	0.86704	3.64104	0.94213
RTADE	1.552	1.218	1.209	0.906					
70%					1.17950	2.13137	0.87547	2.56910	0.95187
80%					1.57142	2.51588	0.86331	2.94753	0.94446
90%					2.23481	3.16573	0.84615	3.58880	0.93092
LAD_2	1.542	1.232	1.208	0.906					
70%					1.17273	2.11241	0.85412	2.53947	0.93969
80%					1.55955	2.49201	0.84272	2.91336	0.93246
90%					2.21413	3.13380	0.82675	3.54717	0.91967

Table 11: KRIs under artificial data for n=300|α_0=1.5, β_0=1.2, a_0=1.2.

Method	α	β	a	b	VaRq(X)	TVaRq(X)	TVq(X)	TMVq(X)	MELq(X)
MLE	1.507	1.206	1.204	0.902					
70%					1.19944	2.16304	0.89912	2.61260	0.96360
80%					1.59587	2.55236	0.88747	2.99610	0.95649
90%					2.26708	3.21083	0.87109	3.64638	0.94375
OLSE	1.510	1.204	1.204	0.906					
70%					1.20128	2.16774	0.90425	2.61987	0.96646
80%					1.59891	2.55821	0.89244	3.00443	0.95930
90%					2.27217	3.21858	0.87579	3.65647	0.94640
ADE	1.505	1.203	1.205	0.899					

70%					1.20470	2.17286	0.90752	2.62661	0.96816
80%					1.60302	2.56401	0.89571	3.01187	0.96099
90%					2.27743	3.22556	0.87910	3.66511	0.94813
RTADE	1.514	1.204	1.205	0.901					
70%					1.20121	2.16863	0.90583	2.62154	0.96742
80%					1.59926	2.55948	0.89389	3.00643	0.96022
90%					2.27325	3.22044	0.87705	3.65897	0.94719
LAD_2	1.505	1.209	1.205	0.901					
70%					1.19921	2.16081	0.89551	2.60857	0.96160
80%					1.59482	2.54931	0.88400	2.99131	0.95449
90%					2.26456	3.20644	0.86783	3.64035	0.94188

Table 12: KRIs under artificial data for n=20|α_o=2.5, β_o=2, a_o=2.5 and b_o=2.

Method	α	β	a	b	VaRq(X)	TVaRq(X)	TVq(X)	TMVq(X)	MELq(X)
MLE	2.925	2.144	2.577	2.022					
70%					0.59789	0.88434	0.07029	0.91948	0.28645
80%					0.72410	0.99778	0.06616	1.03087	0.27369
90%					0.92348	1.18175	0.0614	1.21245	0.25827
OLSE	2.885	2.100	2.580	2.002					
70%					0.61097	0.90545	0.07438	0.94264	0.29448
80%					0.74063	1.02210	0.07005	1.05712	0.28147
90%					0.94562	1.21133	0.06505	1.24386	0.26571
ADE	2.969	2.136	2.561	2.020					
70%					0.59559	0.88389	0.07112	0.91945	0.28830
80%					0.72266	0.99806	0.06690	1.03151	0.27540
90%					0.92341	1.18311	0.06203	1.21413	0.25970
RTADE	2.902	2.092	2.591	2.011					
70%					0.61031	0.90485	0.07434	0.94202	0.29455
80%					0.74006	1.02152	0.06998	1.05650	0.28146
90%					0.94512	1.21069	0.06494	1.24317	0.26557
LAD_2	2.920	2.335	2.553	2.026					
70%					0.57261	0.83622	0.0596	0.86602	0.26361
80%					0.68876	0.9406	0.05616	0.96867	0.25183
90%					0.87199	1.10999	0.05219	1.13608	0.23800

Table 13: KRIs under artificial data for n=50|α_o=2.5, β_o=2, a_o=2.5 and b_o=2.

Method	α	β	a	b	VaRq(X)	TVaRq(X)	TVq(X)	TMVq(X)	MELq(X)
MLE	2.641	2.075	2.525	2.017					
70%					0.60942	0.90032	0.07338	0.93701	0.29090
80%					0.73688	1.01570	0.06946	1.05043	0.27882
90%					0.93908	1.20364	0.06495	1.23611	0.26455
OLSE	2.650	2.043	2.534	2.001					
70%					0.61968	0.91766	0.07695	0.95613	0.29798
80%					0.75027	1.03585	0.07281	1.07225	0.28558
90%					0.95746	1.22830	0.06804	1.26232	0.27084
ADE	2.629	2.048	2.530	2.004					
70%					0.61818	0.91454	0.07618	0.95263	0.29636
80%					0.74801	1.03210	0.07212	1.06815	0.28408
90%					0.95404	1.22358	0.06743	1.25730	0.26955
RTADE	2.715	2.061	2.516	2.015					
70%					0.60741	0.90155	0.07484	0.93897	0.29414
80%					0.73641	1.01820	0.07075	1.05357	0.28179
90%					0.94100	1.20801	0.06603	1.24102	0.26700
LAD_2	2.646	2.124	2.524	2.009					

70%					0.60545	0.89122	0.07080	0.92662	0.28576
80%					0.73071	1.00455	0.06701	1.03805	0.27383
90%					0.92927	1.18913	0.06267	1.22047	0.25986

Table 14: KRIs under artificial data for n=100|α_0=2.5, β_0=2, a_0=2.5 and b_0=2.

Method	α	β	a	b	VaRq(X)	TVaRq(X)	TVq(X)	TMVq(X)	MELq(X)
MLE	2.529	2.042	2.521	2.006					
70%					0.62088	0.91596	0.07583	0.95387	0.29508
80%					0.74994	1.03305	0.07192	1.06901	0.28312
90%					0.95492	1.22408	0.06744	1.25780	0.26916
OLSE	2.626	2.050	2.496	2.013					
70%					0.60953	0.90376	0.07518	0.94135	0.29423
80%					0.73834	1.02050	0.07121	1.05610	0.28216
90%					0.94289	1.21073	0.06663	1.24405	0.26785
ADE	2.626	2.033	2.493	2.012					
70%					0.61151	0.90820	0.07645	0.94642	0.29669
80%					0.74138	1.02592	0.07241	1.06212	0.28453
90%					0.94766	1.21775	0.06775	1.25162	0.27009
RTADE	2.576	2.023	2.516	2.004					
70%					0.62125	0.91998	0.07760	0.95879	0.29874
80%					0.75197	1.03852	0.07354	1.07529	0.28656
90%					0.95960	1.23178	0.06887	1.26622	0.27218
LAD_2	2.620	2.091	2.492	2.018					
70%					0.60245	0.89029	0.07198	0.92627	0.28784
80%					0.72847	1.00448	0.06819	1.03857	0.27601
90%					0.92849	1.19060	0.06383	1.22251	0.26211

Table 15: KRIs under artificial data for n=300|α_0=2.5, β_0=2, a_0=2.5 and b_0=2.

Method	α	β	a	b	VaRq(X)	TVaRq(X)	TVq(X)	TMVq(X)	MELq(X)
MLE	2.528	2.007	2.503	2.002					
70%					0.62362	0.92390	0.07858	0.96319	0.30028
80%					0.75488	1.04309	0.07455	1.08036	0.28820
90%					0.96354	1.23755	0.06990	1.27251	0.27401
OLSE	2.525	2.007	2.504	2.000					
70%					0.62440	0.92482	0.07866	0.96415	0.30042
80%					0.75572	1.04406	0.07462	1.08138	0.28834
90%					0.96448	1.23863	0.06998	1.27362	0.27415
ADE	2.521	2.008	2.504	2.000					
70%					0.62450	0.92478	0.07860	0.96408	0.30028
80%					0.75575	1.04396	0.07457	1.08125	0.28821
90%					0.96439	1.23845	0.06994	1.27342	0.27405
RTADE	2.519	2.003	2.508	1.999					
70%					0.62620	0.92736	0.07906	0.96689	0.30116
80%					0.75784	1.04690	0.07501	1.08440	0.28906
90%					0.96710	1.24195	0.07035	1.27712	0.27485
LAD_2	2.525	2.019	2.502	2.002					
70%					0.62211	0.92058	0.07765	0.95940	0.29847
80%					0.75258	1.03904	0.07367	1.07588	0.28646
90%					0.95996	1.23235	0.06909	1.26689	0.27239

7. Checking model applicability

We will evaluate the performance of the ExEE distribution by comparing it with several other competitive models, including: exponential (E), Odd Lindley exponential (OLE), Marshall-Olkin exponential (MOE), Moment exponential (ME), Logarithmic Burr-Hatke exponential (LBHE), Generalized Marshall-Olkin exponential (GMOE), Beta exponential (BE), Marshall-Olkin Kumaraswamy exponential (MOKwE), Kumaraswamy exponential (KwE), Burr X exponential (BrXE), and Kumaraswamy Marshall-Olkin exponential (KwMOE). To compare these models, we will use the Cramér-Von Mises (C*), Anderson-Darling (A*), and Kolmogorov-Smirnov (KS) statistics. Additionally, for a more comprehensive evaluation, we will include five other goodness-of-fit measures: the Akaike Information

Criterion (C_1), Bayesian Information Criterion (C_2), Consistent Akaike Information Criterion (C_3), and Hannan-Quinn (C_4).

7.1 Failure data

The failure (or relief) times data have recently been analyzed by Ibrahim et al. (2020) and Al-Babtain et al. (2020). In Table 16, we present the maximum likelihood estimates (MLEs) along with their standard errors (SEs) and the corresponding confidence intervals (CIs). This table provides a detailed overview of the estimated parameters and the precision of these estimates. Table 17 includes a range of goodness-of-fit measures and statistical tests used to evaluate the models. Specifically, it lists the C_1, C_2 ,C_3 ,C_4, A*, C*, K.S., and the associated p-value. These measures and statistics help assess the fit of the models to the data. Figure 1 illustrates three different plots for analyzing the relief times data. The box plot displays the distribution of relief times, showing the median, quartiles, and potential outliers. The box plot helps identify the central tendency and variability of the data, as well as any extreme values or outliers that may be present. The Quantile-Quantile (Q-Q) plot compares the quantiles of the relief times data against the quantiles of a theoretical normal distribution. This plot assesses whether the data follows a normal distribution by plotting the actual data quantiles against the expected normal quantiles. Deviations from the reference line indicate deviations from normality. The kernel density plot is used to assess the goodness-of-fit of the data to an exponential distribution. It plots the ordered relief times against their expected values if they were drawn from an exponential distribution. The reference line helps evaluate how well the observed data conforms to the expected distribution. Together, these plots provide a comprehensive overview of the relief times data, allowing for a thorough examination of its distribution and fit to theoretical models.

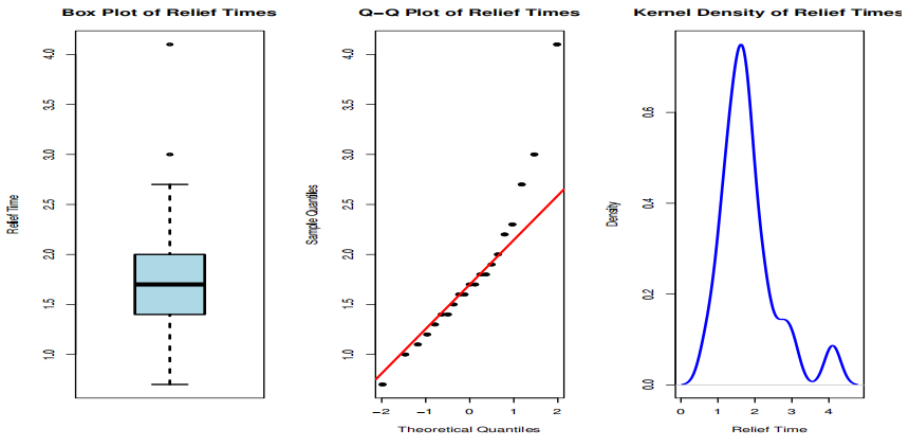

Figure 1: Box plot, QQ plot, kernel plot for the relief times data.

Figure 2 provides visual representations related to the analysis. On the right side of the figure, the estimated probability density function (E-PDF) is displayed, illustrating the distribution of the relief times data. On the left side, the Kaplan-Meier survival plot is shown, which graphically represents the survival function and provides insights into the time until failure or relief events. Based on Table 17, we conclude that the ExEE model demonstrates superior performance compared to the other models based on the results presented in Table 17. ExEE has the lowest values for the C 1 , C 2 ,C 3 ,C 4 , A*, C*, K.S., and the associated p-values (0.8417), suggesting that it's fit to the data is not significantly different from the perfect model, thus confirming its excellent performance in fitting the relief times data. The ExEE model not only achieves the best scores across the various goodness-of-fit measures but also maintains the most favorable statistical significance, indicating it is the best model for the given relief times data.

Table 16: MLEs and SEs for the relief times data.

Models		MLEs and SEs
E|b	MLE	0.526
	SE	(0.117)
OLE|b	MLE	0.6044
	SE	(0.0535)
ME|b	MLE	0.950
	SE	(0.150)
LBHE|b	MLE	0.5263
	SE	(0.118)
MOKwE|α,β,λ,b	MLE	54.474, 2.316
	SE	(0.332), (57.85), (0.7), (1.8)

BrXE|a,b	MLE	8.868, 34.826, 0.299, 4.899
	SE	(0.33), (0.03)
ExEE|α,β,a,b	MLE	0.0125, 0.88, 2.78, 2.57
	SE	(0.028), (0.944), (5.549), (2.55)

Table 17: C_1, C_2, C_3, C_4, A*, C*, K.S. and (p-value) for the relief times data.

Models	C_1, C_2, C_3, C_4	A*	C*	K.S. and (p-value)
E	67.70, 68.70, 67.89, 68.90	4.60	0.961	0.44(<0.01)
OLE	49.12, 50.14, 49.33, 49.34	1.32	0.223	0.85(<0.001)
ME	54.32, 55.31, 54.54, 54.50	2.76	0.537	0.32(0.1)
LBHE	67.70, 68.70, 67.89, 67.90	0.62	0.103	0.44(<0.001)
BrXE	48.13, 50.15, 48.83, 48.52	1.39	0.244	0.248(0.171)
ExEE	44.72, 48.71 47.39, 45.50	0.67	0.113	0.13785(0.8417)

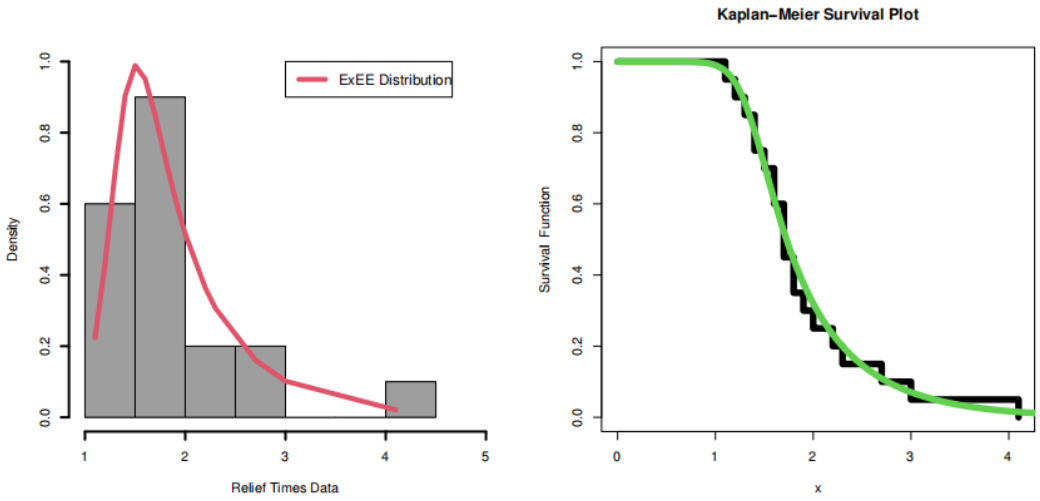

Figure 2: E-PDF and Kaplan-Meier survival plot for relief times data.

7.2 Survival data

The second data set consists of survival times (in days) for 72 guinea pigs that were infected with virulent tubercle bacilli. This data was initially observed and reported by Bjerkedal (1960). More recently, the data has been reanalyzed by Ibrahim et al. (2020) and Al-Babtain et al. (2020) to gain further insights. In Table 18, we present the MLEs for the parameters, along with their SEs. This table provides a detailed summary of the estimated parameters and their precision for the survival times data. Table 19 contains a range of goodness-of-fit measures and statistical tests used to assess the models applied to the survival times data. This includes the C_1, C_2, C_3, C_4, A*, C*, K.S., and the associated p-value. These statistics are crucial for evaluating how well each model fits the data. Figure 3 gives the box plot, Q-Q plot and kernel plot for the survival times data. Figure 4 provides visual representations of the analysis. On the right side, the E-PDF is shown, illustrating the distribution of the survival times. On the left side, the Kaplan-Meier survival plot is displayed, which graphically represents the survival function and provides insights into the time until failure or the end of the study period for the guinea pigs.

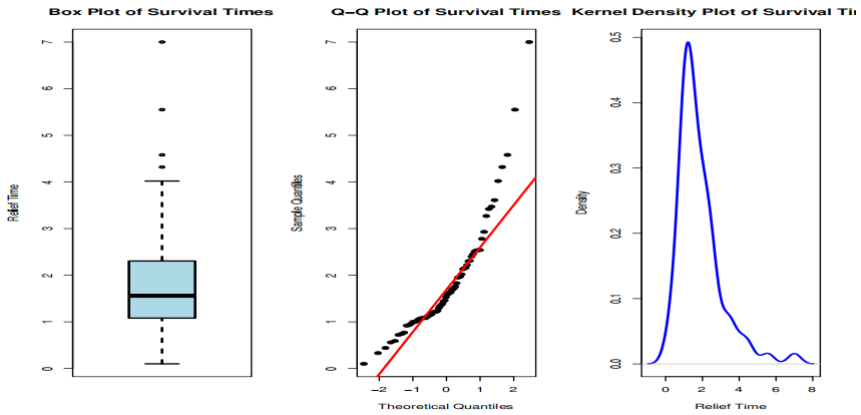

Figure 3: Box plot, QQ plot, kernel plot for the survival times data.

Table 18: MLEs and SEs for the survival times data.

Models		MLEs and SEs
E|b	MLE	0.540
	SE	(0.063)
OLE|b	MLE	0.3815
	SE	(0.021)
ME|b	MLE	0.925
	SE	(0.077)
LBHE|b	MLE	0.54
	SE	(0.064)
MOE|α,b	MLE	8.78, 1.38
	SE	(3.56), (0.19)
BrXE|a,b	MLE	0.48, 0.21
	SE	(0.060), (0.012)
GMOE|λ,α,b	MLE	0.18, 47.64, 4.47
	SE	(0.07), (44.9), (1.33)
KwE|a,β,b	MLE	3.304, 1.100, 1.037
	SE	(1.106), (0.764), (0.614)
BE|a,β,b	MLE	0.807, 3.461, 1.331
	SE	(0.696), (1.003), (0.860)
MOKwE|α,β,λ,b	MLE	0.008, 2.716, 1.986, 0.099
	SE	(0.002), (1.316), (0.784), (0.05)
KwMOE|α,β,λ,b	MLE	0.373, 3.478, 3.306, 0.299
	SE	(0.136), (0.861), (0.779), (1.112)
ExEE|α,β,a,b	MLE	0.441, 0.697, 3.17, 1.42
	SE	(1.01), (0.8), (1.28), (1.52)

Table 19: C_1, C_2, C_3, C_4, A*, C*, K.S. and (p-value) for survival times data.

Models	C_1, C_2, C_3, C_4	A*	C*	K.S. and (p-value)
E	234.60, 236.90, 234.68, 235.55	6.53	1.25	0.3(0.06)
OLE	229.13, 231.43, 229.21, 230.11	1.94	0.33	0.5(<0.001)
ME	210.40, 212.68, 210.45, 211.30	1.52	0.25	0.15(0.13)
LBHE	234.63, 236.92, 234.71, 235.51	0.71	0.115	0.28(<0.001)
MOE	210.37, 214.93, 210.52, 212.17	1.18	0.17	0.10(0.43)
GMOE	210.54, 217.38, 210.89, 213.24	1.02	0.16	0.09(0.5)
KwE	209.42, 216.24, 209.77, 212.12	0.74	0.11	0.09(0.5)
BE	207.37, 214.21, 207.73, 210.09,	0.98	0.15	0.11(0.34)
MOKwE	209.44, 218.56, 210.04, 213.04,	0.79	0.12	0.10(0.44)
KwMOE	207.82, 216.94, 208.42, 211.42	0.61	0.11	0.09(0.5)
BrXE	235.31, 239.92, 235.53, 237.14	2.90	0.52	0.22(0.002)
ExEE	207.28, 216.38,207.87, 210.90	0.59	0.095	0.09(0.6065)

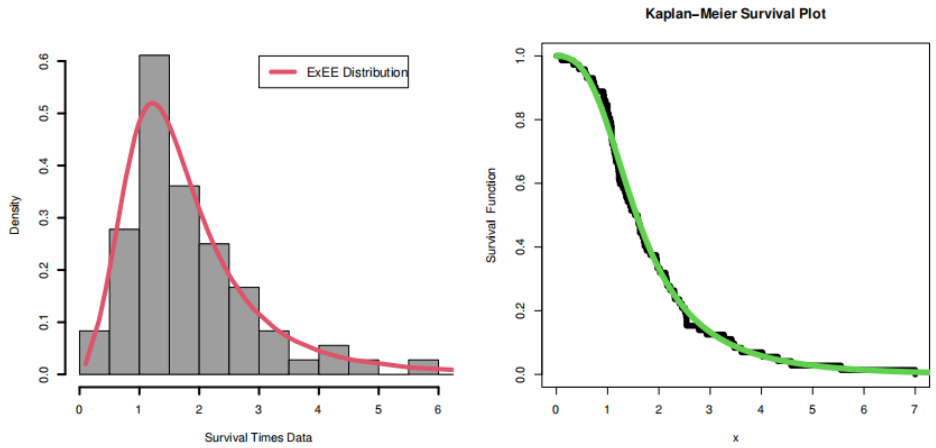

Figure 4: E-PDF and Kaplan-Meier survival plot for survival times data.

8. Reliability and risk analysis

Recent research has significantly contributed to the development of novel distribution models tailored for risk analysis. Hamed et al. (2022) introduced a new compound model, which incorporates properties and copulas to better handle negatively skewed insurance claims data. Similarly, Yousof et al. (2023b) proposed a new reciprocal exponential extension specifically for modeling extreme values in insurance data. Shrahili, Elbatal, and Yousof (2021) developed an asymmetric density function tailored for claim-size data, addressing the challenge of predicting and analyzing bimodal data effectively. This approach is critical for capturing the complexity of claim-size distributions (Shrahili et al., 2021). Furthermore, Yousof et al. (2023) explored a bimodal heavy-tailed Burr XII model and applied multiple methods to assess risk in insurance data. Their work highlights the importance of accommodating multiple modes and heavy tails to provide accurate risk assessments (Yousof et al., 2023a,c,d,e,f). Khedr et al. (2023) further developed a new family of compound probability distributions with applications to reinsurance revenue data, emphasizing the importance of copulas and risk analysis in managing complex insurance data. Ibrahim et al. (2023) examined both Bayesian and non-Bayesian methods under left-skewed insurance data, introducing a novel compound reciprocal Rayleigh extension. Similarly, Hashempour et al. (2023b) proposed a new Lindley extension for bimodal right-skewed precipitation data, offering insights into estimation and risk assessment in various contexts. Yousof et al. (2024) analyzed a discrete claims model for inflated and over-dispersed automobile claims frequencies, demonstrating the model's applicability in actuarial risk analysis. Alizadeh et al. (2024) introduced an extended Gompertz model for statistical threshold risk analysis, reflecting ongoing efforts to refine and expand risk modeling techniques. In this section, we delve into the application of insurance risk measurement and analysis criteria within the realms of engineering and reliability.

8.1 Risk analysis for extreme failures

8.1.1 The non-parametric Hill estimator for extreme failures

The non-parametric Hill estimator is crucial for analyzing extreme failures, as it provides a robust measure of tail heaviness without assuming a specific distribution. It helps quantify the likelihood of catastrophic events, aiding in risk assessment and mitigation strategies. By focusing on the most extreme values, it enables better predictions of rare but severe failures in fields like finance, engineering, and climate science. Its flexibility makes it essential for stress testing, insurance modeling, and extreme event forecasting. Figure 5 presents two key visualizations used in extreme value analysis to assess the tail behavior of failure data. The Hill estimator plot (right) depicts how the estimated tail index varies as more extreme observations are included. Initially, the estimator is high, indicating the presence of severe, infrequent failures with potentially heavy-tailed characteristics. However, as additional top-order statistics are incorporated, the estimator declines, suggesting a lighter tail, meaning that the probability of extreme failures diminishes at higher thresholds. The stability plot (left), shown in a log-log scale, provides further insight into the convergence behavior of the tail index. The downward trend in this plot implies that while extreme failures exist, their impact decreases as more data is considered, reinforcing the presence of an exponentially decaying tail rather than a power-law behavior. The fluctuations observed in both plots suggest variability in the occurrence of extreme failures, necessitating robust risk assessment strategies such as stress testing, threshold-based monitoring, and extreme value modeling (EVT) to better predict and mitigate high-impact risks. The Hill estimator plots indicate the presence of

extreme failures, initially showing a high tail index (~6), suggesting rare but severe events. As more extreme values are considered, the tail index decreases, implying a lighter tail and diminishing probability of catastrophic failures. The fluctuations in the Hill estimator highlight variability in extreme risks, necessitating robust stress testing and adaptive risk management strategies. The log-log stability plot further confirms an exponentially decaying tail, suggesting that while extreme failures exist, their frequency declines rapidly. Effective risk mitigation should include EVT-based modeling, threshold monitoring, and dynamic scenario analysis to prevent systemic breakdowns.

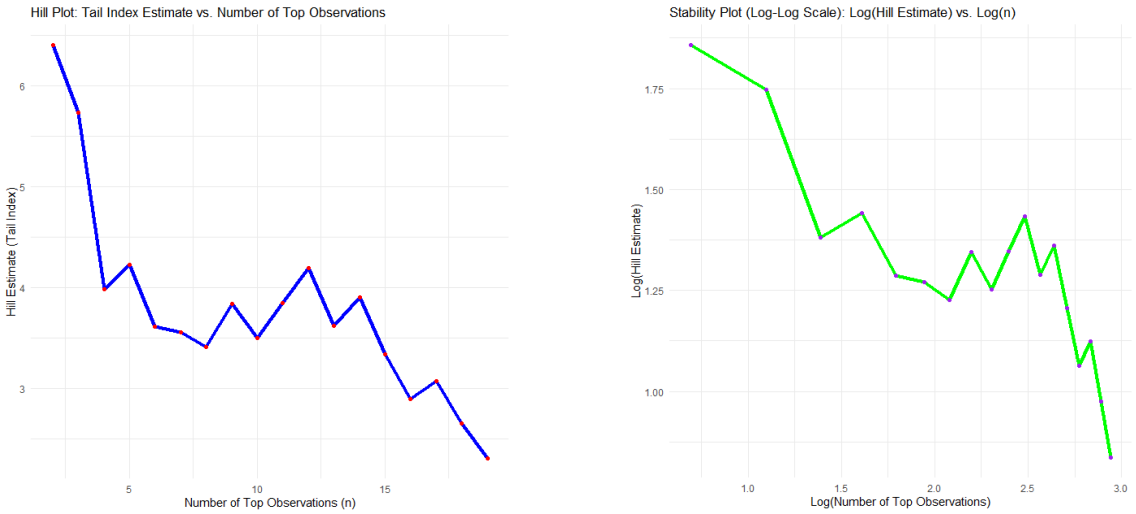

Figure 5: Hill estimator plot (right) and stability plot (left) for the extreme failures.

8.1.2 Risk assessment for extreme failures

Using KRIs with failure times data, particularly in the context of survival analysis or reliability engineering, can offer important insights and benefits. KRIs applied to failure times data enables the quantification of time-dependent risk. By calculating VaR over different time horizons, one can understand how the risk of experiencing the event (e.g., system failure) changes over time. This is particularly useful for predicting and managing risks associated with time-critical events. In reliability engineering and maintenance planning, understanding the distribution of failure times and associated risks is crucial. VaR can assist in optimizing maintenance schedules and resource allocation by identifying critical time periods where the risk of failure is highest. This helps in prioritizing preventive maintenance activities and minimizing potential downtime. In this subsection, we analyze the dataset which represents failure time data related to relief times (in minutes) experienced by patients who have received an analgesic. This type of data is commonly analyzed in survival analysis, a statistical field focused on studying the time until specific events, such as failure or death, occur (see Gross and Clark (1975)).

Table 20 provides the KRIs under failure time due to five different estimation methods. Understanding these risk measures is crucial for effective risk management, VaRq $(X|\underline{\hat{\boldsymbol{\Psi}}})$ provides a baseline threshold for potential failure, TVaRq $(X|\underline{\hat{\boldsymbol{\Psi}}})$, TVq $(X|\underline{\hat{\boldsymbol{\Psi}}})$, and TMVq $(X|\underline{\hat{\boldsymbol{\Psi}}})$ offer insights into tail risk and extreme failure and finally, MELq $(X|\underline{\hat{\boldsymbol{\Psi}}})$ helps in assessing average expected failures. In view of Table 20, we can highlight the following main results:

1) Method (MLE): As the quantile level increases (from 70% to 90%), the estimated VaRq $(X|\underline{\hat{\boldsymbol{\Psi}}})$, TVaRq $(X|\underline{\hat{\boldsymbol{\Psi}}})$, TVq $(X|\underline{\hat{\boldsymbol{\Psi}}})$, and TMVq $(X|\underline{\hat{\boldsymbol{\Psi}}})$ values also increase, indicating higher potential losses at higher confidence levels. The MELq $(X|\underline{\hat{\boldsymbol{\Psi}}})$ values decrease as the quantile level increases, reflecting the average expected loss under more extreme failures.
2) Method (OLSE): Similar to the MLE method, the values of VaRq $(X|\underline{\hat{\boldsymbol{\Psi}}})$, TVaRq $(X|\underline{\hat{\boldsymbol{\Psi}}})$, TVq $(X|\underline{\hat{\boldsymbol{\Psi}}})$, and TMVq $(X|\underline{\hat{\boldsymbol{\Psi}}})$ increase as the quantile level increases from 70% to 90%. This signifies higher potential losses or tail risk at higher confidence levels. The MELq $(X|\underline{\hat{\boldsymbol{\Psi}}})$ values decrease with increasing quantile levels, indicating lower expected losses under more extreme failures.
3) Method (ADE): As the quantile level increases from 70% to 90%, the values of VaRq $(X|\underline{\hat{\boldsymbol{\Psi}}})$, TVaRq $(X|\underline{\hat{\boldsymbol{\Psi}}})$, TVq $(X|\underline{\hat{\boldsymbol{\Psi}}})$, and TMVq $(X|\underline{\hat{\boldsymbol{\Psi}}})$ generally increase. This indicates higher estimated losses or tail risks at higher

confidence levels. The MELq $(X|\widehat{\underline{\boldsymbol{\Psi}}})$ values decrease with increasing quantile levels, suggesting lower expected losses under more extreme failures.

4) Method (RTADE): As the quantile level increases from 70% to 90%, the values of VaRq $(X|\widehat{\underline{\boldsymbol{\Psi}}})$, TVaRq $(X|\widehat{\underline{\boldsymbol{\Psi}}})$, TVq $(X|\widehat{\underline{\boldsymbol{\Psi}}})$, and TMVq $(X|\widehat{\underline{\boldsymbol{\Psi}}})$ generally increase. This signifies higher estimated losses or tail risks at higher confidence levels. The MELq $(X|\widehat{\underline{\boldsymbol{\Psi}}})$ values decrease with increasing quantile levels, indicating lower expected losses under more extreme failures.
5) Method (LAD 2): As the quantile level increases from 70% to 90%, the values of VaRq $(X|\widehat{\underline{\boldsymbol{\Psi}}})$, TVaRq $(X|\widehat{\underline{\boldsymbol{\Psi}}})$, TVq $(X|\widehat{\underline{\boldsymbol{\Psi}}})$, and TMVq $(X|\widehat{\underline{\boldsymbol{\Psi}}})$ generally increase. This signifies higher estimated losses or tail risks at higher confidence levels. The MELq $(X|\widehat{\underline{\boldsymbol{\Psi}}})$ values decrease with increasing quantile levels, indicating lower expected losses under more extreme failures.
6) Based on the criteria of larger VaRq, TVaRq, TVq, TMVq and MELq values, and smaller MELq values, the RTADE method appears to be a favorable choice, since it provides higher VaRq, TVaRq, TVq, TMVq and MELq values, indicating a more robust estimation of tail risks and extreme events. Demonstrates lower MELq values, suggesting reduced expected losses under extreme failures.

Table 20: KRIs under failure time.

Method	VaRq$(X\|\widehat{\underline{\boldsymbol{\Psi}}})$	TVaRq$(X\|\widehat{\underline{\boldsymbol{\Psi}}})$	TVq$(X\|\widehat{\underline{\boldsymbol{\Psi}}})$	TMVq$(X\|\widehat{\underline{\boldsymbol{\Psi}}})$	MELq$(X\|\widehat{\underline{\boldsymbol{\Psi}}})$
MLE|q					
70%	2.06188	2.69573	0.39517	2.89331	0.63385
80%	2.32069	2.95223	0.39250	3.14848	0.63154
90%	2.76122	3.38858	0.38840	3.58278	0.62736
OLSE|q					
70%	1.99954	2.36432	0.11512	2.42188	0.36478
80%	2.16256	2.50787	0.10975	2.56275	0.34531
90%	2.41111	2.74104	0.10574	2.79391	0.32993
ADE|q					
70%	2.06893	2.47928	0.14612	2.55235	0.41036
80%	2.25204	2.64085	0.13949	2.71059	0.38881
90%	2.53165	2.90354	0.13460	2.97083	0.37189
RTADE|q					
70%	2.10314	2.60827	0.22508	2.72081	0.50513
80%	2.32676	2.80764	0.21631	2.91579	0.48088
90%	2.67086	3.13354	0.21055	3.23881	0.46268
LAD_2|q					
70%	1.93138	2.21054	0.06649	2.24379	0.27916
80%	2.05696	2.32018	0.06302	2.35169	0.26322
90%	2.24724	2.49743	0.06027	2.52757	0.25019

8.1.3 PORT-VaRq analysis for failure times

Following Alizadeh et al. (2024), Shehata et al. (2024a), Khan et al. (2024), Aljadani et al. (2024a,b) Yousof et al. (2024a,b) and Das et al. (2025), the PORT-VaRq analysis is essential in reliability engineering as it identifies extreme failure events, improving risk assessment and system durability. By analyzing failures beyond different thresholds, it helps predict catastrophic failures and optimize maintenance strategies. The increasing peaks at lower VaRq levels highlight the concentration of extreme failures, aiding in failure prediction and system design. This approach enhances safety, reduces downtime, and improves decision-making in reliability management. The PORT-VaRq analysis for failure times presented in Table 21 provides insights into the behavior of extreme failure events beyond the given VaRq thresholds. As the confidence level (CL) increases from 55% to 95%, the VaRq threshold gradually decreases from 1.700 to 1.195, leading to an increase in the number of peaks above VaRq from 9 to 19. This trend aligns with the expected tail risk behavior, where lower thresholds capture more extreme observations. The data shows that between CL of 55% (VaRq = 1.7) and CL of 65% (VaRq = 1.6), the number of peaks increases moderately (from 9 to 12), indicating that failure events are relatively concentrated in this range. However, beyond CL of 70% (VaRq = 1.57), the number of peaks rises more steadily, reaching 19 at CL of 95%, demonstrating that more extreme failure

times become significant at higher confidence levels. The relatively small differences in peak counts at some levels (e.g., 15 peaks at both CL of 75% and CL of 80%) suggest stability in failure event distribution within this range.

Table 21: PORT-VaRq analysis for failure times

CL	VaRq	Number of Peaks Above VaRq
55%	1.700	9
60%	1.660	12
65%	1.600	12
70%	1.570	14
75%	1.475	15
80%	1.400	15
85%	1.385	17
90%	1.290	18
95%	1.195	19

Figure 6 presents histograms that illustrate the distribution of failure times, accompanied by VaR thresholds and related peaks. Each histogram provides a visual representation of how frequently different failure times occur, with bars indicating the frequency of failure events within specific time intervals. The inclusion of VaR thresholds as horizontal dashed lines at varying confidence levels (55% to 95%) allows for a comparative analysis of risk across different tolerance levels. These thresholds represent critical points beyond which failures are considered rare or extreme, and their positions shift downward as the confidence level increases, reflecting stricter criteria for defining risk. Red markers (peaks) highlight specific failure times that exceed the corresponding VaR threshold, providing insight into the most significant or outlier events in the dataset. By examining the number and distribution of these peaks across different confidence levels, analysts can assess the severity and frequency of extreme failure scenarios. Figure 7 below employs KDEs to offer a smooth, continuous representation of the same data. Both figures include VaR thresholds and related peaks, allowing for a detailed comparison of typical failure patterns and extreme events across different confidence levels.

The results indicate a clear relationship between the confidence level and the number of peaks above VaR, demonstrating expected tail risk behavior. At CL of 55%, VaR is 1.7, capturing only 9 peaks, with a median peak of 2.2 and a mean of 2.422. As the confidence level increases to CL of 75%, VaR drops to 1.475, increasing the number of peaks to 15, with the median shifting to 1.8 and the mean decreasing to 2.107. By CL of 95%, VaR reaches 1.195, capturing 19 peaks, where the median falls to 1.7, and the mean further declines to 1.942. The maximum peak remains constant at 4.1 across all levels, while the minimum peak varies slightly, decreasing from 1.8 (CL of 55%) to 1.2 (CL of 95%). This smooth transition confirms that as the confidence level rises, more tail events are included, with lower VaR thresholds allowing for a broader distribution of extreme values. Together, Figure 6, Figure 7 and Table 21 present the overall PORT-VaRq analysis for failure times data.

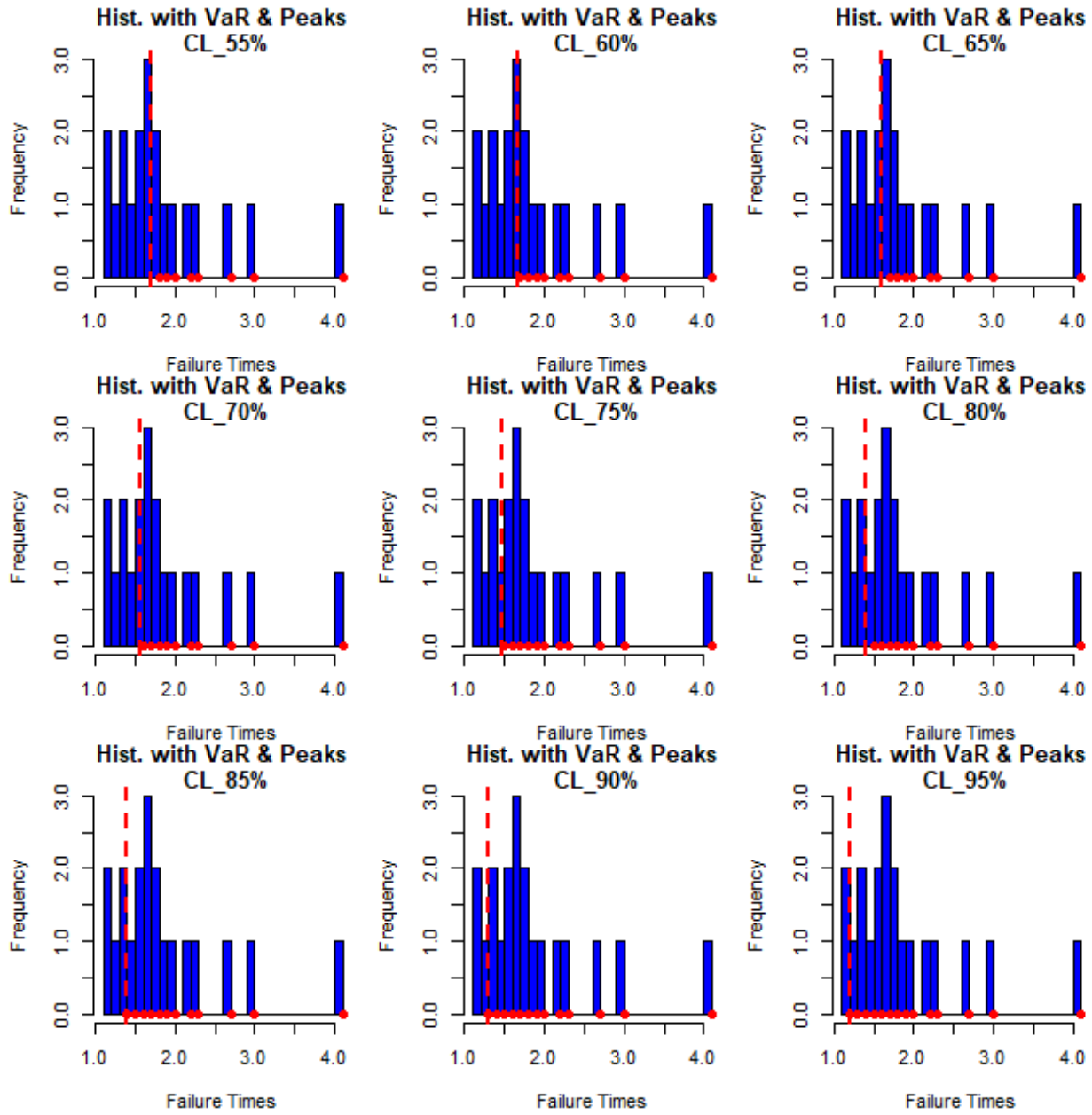

Figure 6: Histograms with VaR and related peaks for the failure times.

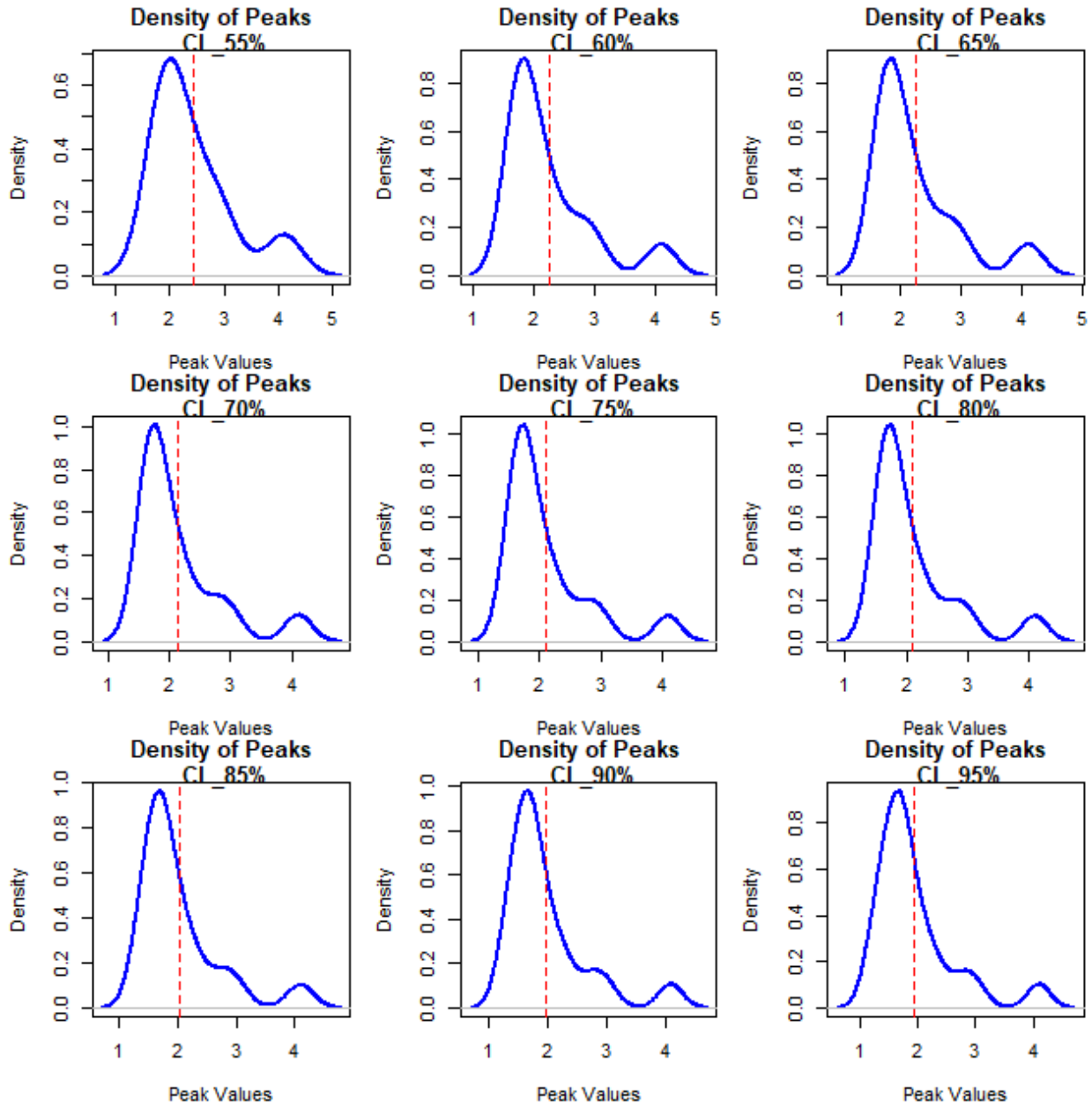

Figure 7: Kernel densities with VaR and related peaks for the failure times.

8.2 Risk analysis for extreme survivals

8.2.1 The nonparametric Hill estimator for extreme survivals

Figure 8 presents two key statistical tools used in extreme value analysis to assess the behavior of extreme survivals, where rare but significant events persist over time. In extreme value analysis, understanding extreme survivals, cases where rare but significant events persist, is crucial for risk assessment and system resilience. The given Hill estimator plot provides insights into the behavior of the tail index as more extreme data points are incorporated. Initially, the tail index is very high (~7.5), indicating the presence of extreme survival events with heavy-tail characteristics. As more data is included, the estimator declines, suggesting that while extreme survivals exist, their probability reduces gradually rather than disappearing abruptly.

The fluctuations in the middle of the plot highlight variability in extreme survival patterns, implying that some events persist longer than expected. This behavior necessitates robust survival analysis models, stress testing, and scenario

planning to manage risks effectively. The tail index's overall downward trend suggests a progressive reduction in risk, reinforcing the need for dynamic monitoring systems to track and adapt to rare but impactful survivals.

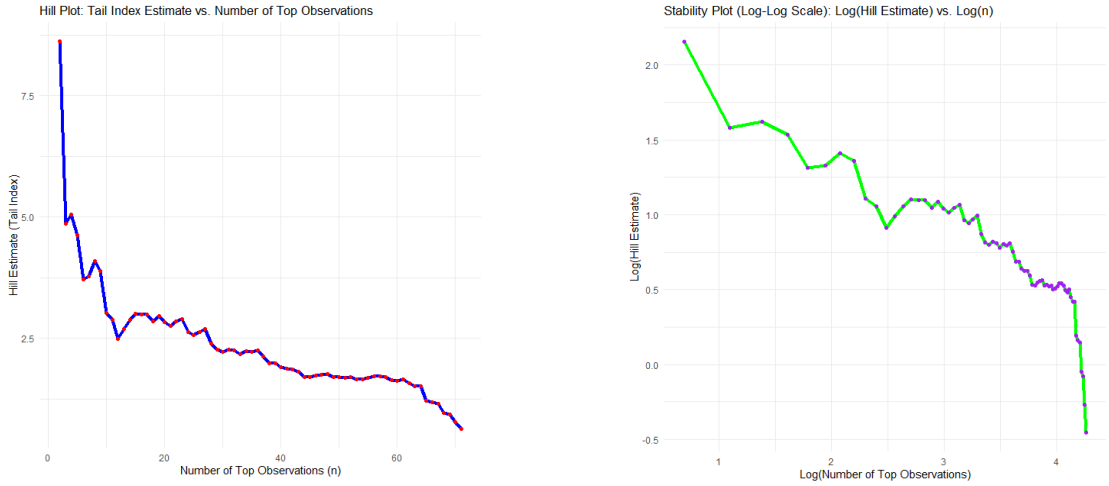

Figure 8: Hill estimator plot (right) and stability plot (left) for the extreme survivals.

8.2.2 Risk assessment for extreme survivals

Table 22 provides the KRIs under survival time due to five different estimation methods. Understanding these risk measures is crucial for effective risk management, VaRq $(X|\underline{\hat{\Psi}})$ provides a baseline threshold for potential failure, TVaRq $(X|\underline{\hat{\Psi}})$, TVq $(X|\underline{\hat{\Psi}})$, and TMVq $(X|\underline{\hat{\Psi}})$ offer insights into tail risk and extreme failure and finally, MELq $(X|\underline{\hat{\Psi}})$ helps in assessing average expected failures. In view of Table 21, we can highlight the following main results:

1) For the MLE method: As the quantile level increases from 70% to 90%, the values of VaRq $(X|\underline{\hat{\Psi}})$, TVaRq $(X|\underline{\hat{\Psi}})$, TVq $(X|\underline{\hat{\Psi}})$, and TMVq $(X|\underline{\hat{\Psi}})$ generally increase. This indicates higher estimated losses or tail risks at higher confidence levels. The MELq $(X|\underline{\hat{\Psi}})$ values decrease with increasing quantile levels, suggesting lower expected losses under more extreme survival threshold.
2) For the OLSE: As the quantile level increases from 70% to 90%, the values of VaRq $(X|\underline{\hat{\Psi}})$, TVaRq $(X|\underline{\hat{\Psi}})$, TVq $(X|\underline{\hat{\Psi}})$, and TMVq $(X|\underline{\hat{\Psi}})$ generally increase. This indicates higher estimated losses or tail risks at higher confidence levels. The MELq $(X|\underline{\hat{\Psi}})$ values decrease with increasing quantile levels, suggesting lower expected losses under more extreme survival threshold.
3) For the ADE: As the quantile level (confidence level) increases from 70% to 90%, the values of VaRq $(X|\underline{\hat{\Psi}})$, TVaRq $(X|\underline{\hat{\Psi}})$, TVq $(X|\underline{\hat{\Psi}})$, and TMVq $(X|\underline{\hat{\Psi}})$ generally increase. This suggests higher estimated losses or tail risks at higher confidence levels. The MELq $(X|\underline{\hat{\Psi}})$ values decrease with increasing quantile levels, indicating lower expected losses under more extreme survival threshold.
4) For the RADE: As the quantile level (confidence level) increases from 70% to 90%, the values of VaRq $(X|\underline{\hat{\Psi}})$, TVaRq $(X|\underline{\hat{\Psi}})$, TVq $(X|\underline{\hat{\Psi}})$, and TMVq $(X|\underline{\hat{\Psi}})$ generally increase. This suggests higher estimated losses or tail risks at higher confidence levels. The MELq $(X|\underline{\hat{\Psi}})$ values decrease with increasing quantile levels, indicating lower expected losses under more extreme survival threshold.
5) For the LAD 2 and as the quantile level (confidence level) increases from 70% to 90%, the values of VaRq $(X|\underline{\hat{\Psi}})$, TVaRq $(X|\underline{\hat{\Psi}})$, TVq $(X|\underline{\hat{\Psi}})$, and TMVq $(X|\underline{\hat{\Psi}})$ generally increase. This suggests higher estimated losses or tail risks at higher confidence levels. The MELq $(X|\underline{\hat{\Psi}})$ values decrease with increasing quantile levels, indicating lower expected losses under more extreme survival threshold.
6) For VaRq $(X|\underline{\hat{\Psi}})$ and TVaRq $(X|\underline{\hat{\Psi}})$: RTADE consistently shows higher values across all quantile levels (70%, 80%, 90%), indicating a more conservative estimate of risk exposure compared to other methods. For TVq $(X|\underline{\hat{\Psi}})$ and TMVq $(X|\underline{\hat{\Psi}})$: RTADE also exhibits relatively higher values, suggesting a more robust capture of tail risk variability beyond the VaR threshold. For MELq $(X|\underline{\hat{\Psi}})$: While MELq $(X|\underline{\hat{\Psi}})$ values vary across methods and quantile levels, RTADE generally maintains competitive performance with relatively lower expected losses compared to other methods.

Table 22: KRIs under survival times.

Method	VaRq($X\|\hat{\underline{\Psi}}$)	TVaRq($X\|\hat{\underline{\Psi}}$)	TVq($X\|\hat{\underline{\Psi}}$)	TMVq($X\|\hat{\underline{\Psi}}$)	MELq($X\|\hat{\underline{\Psi}}$)
MLE|q					
70%	2.09778	2.96028	0.69698	3.30877	0.86250
80%	2.46634	3.30460	0.68418	3.64669	0.83827
90%	3.06226	3.87689	0.68445	4.21911	0.81463
OLSE|q					
70%	2.09514	2.90025	0.44398	3.12224	0.80511
80%	2.50248	3.20351	0.38318	3.39510	0.70103
90%	3.03938	3.65585	0.33359	3.82264	0.61647
ADE|q					
70%	2.09347	2.95753	0.58802	3.25154	0.86407
80%	2.49168	3.29517	0.53346	3.56190	0.80349
90%	3.09317	3.82505	0.47579	4.06294	0.73188
RTADE|q					
70%	2.09894	2.99451	0.59566	3.29234	0.89558
80%	2.52865	3.33963	0.52851	3.60388	0.81098
90%	3.14307	3.86841	0.46694	4.10188	0.72534
LAD_2|q					
70%	2.02407	2.80634	0.57995	3.09632	0.78227
80%	2.35580	3.11921	0.57172	3.40507	0.76341
90%	2.89094	3.64365	0.57006	3.92868	0.75271

8.2.3 PORT-VaR analysis for survival times

The PORT-VaRq analysis for survival times, presented in Table 23, tracks the behavior of survival events exceeding varying thresholds of VaRq across different CL. As the confidence level increases from 55% to 95%, the VaRq threshold gradually decreases from 1.3885 to 0.5765, while the number of peaks above the threshold increases from 40 to 68. This pattern indicates that more extreme survival times are captured as the threshold becomes lower, suggesting a broader distribution of survival events at higher confidence levels. The number of peaks increases steadily with the decrease in VaRq, reflecting a shift towards capturing more outlier survival times as confidence levels increase. For instance, from 55% (VaRq = 1.3885) to 95% (VaRq = 0.5765), the number of peaks increases almost linearly, from 40 to 68, illustrating that lower thresholds incorporate more survival events. This result is consistent with expectations, as lowering the VaRq threshold captures more of the tail distribution, allowing for a better understanding of extreme survival times.

Table 23: PORT-VaRq analysis for survival times

CL	VaRq	Number of Peaks Above VaRq
55%	1.3885	40
60%	1.2640	43
65%	1.2085	47
70%	1.1360	50
75%	1.0800	53
80%	1.0540	57
85%	0.9860	61
90%	0.7850	64
95%	0.5765	68

Figure 9 below presents a series of histograms that illustrate the distribution of survival times, along with Value-at-VaR thresholds and related peaks at varying confidence levels (55% to 95%). This figure is analogous to previous

analyses of failure times but focuses on survival times, which likely represent the duration before an event occurs or the time until failure. Below is a detailed expansion of the figure, highlighting its key components, patterns, and insights. The results again show a clear pattern where a decrease in the VaR threshold leads to an increase in the number of peaks above it. At CL of 55%, VaR is 1.3885, capturing 40 peaks, with a median of 2.19 and a mean of 2.551. As the confidence level rises to 75%, VaR drops to 1.08, increasing peaks to 53, while the median decreases to 1.95 and the mean to 2.223. By 95%, the VaR further declines to 0.5765, capturing 68 peaks, with a median of 1.615 and a mean of 1.938. The maximum peak remains constant at 7.0, while the minimum peak follows a declining trend, dropping from 1.39 (CL of 55%) to 0.59 (CL of 95%). The smooth progression in peak counts and VaR values confirms the expected risk distribution behavior, with increasing confidence levels incorporating more tail events and broadening the range of extreme values. Finally, Figure 10 shows the Kernel densities with VaR and related peaks for the survival times. Together, Figure 9, Figure 10 and Table 23 present the overall PORT-VaRq analysis for survival times data.

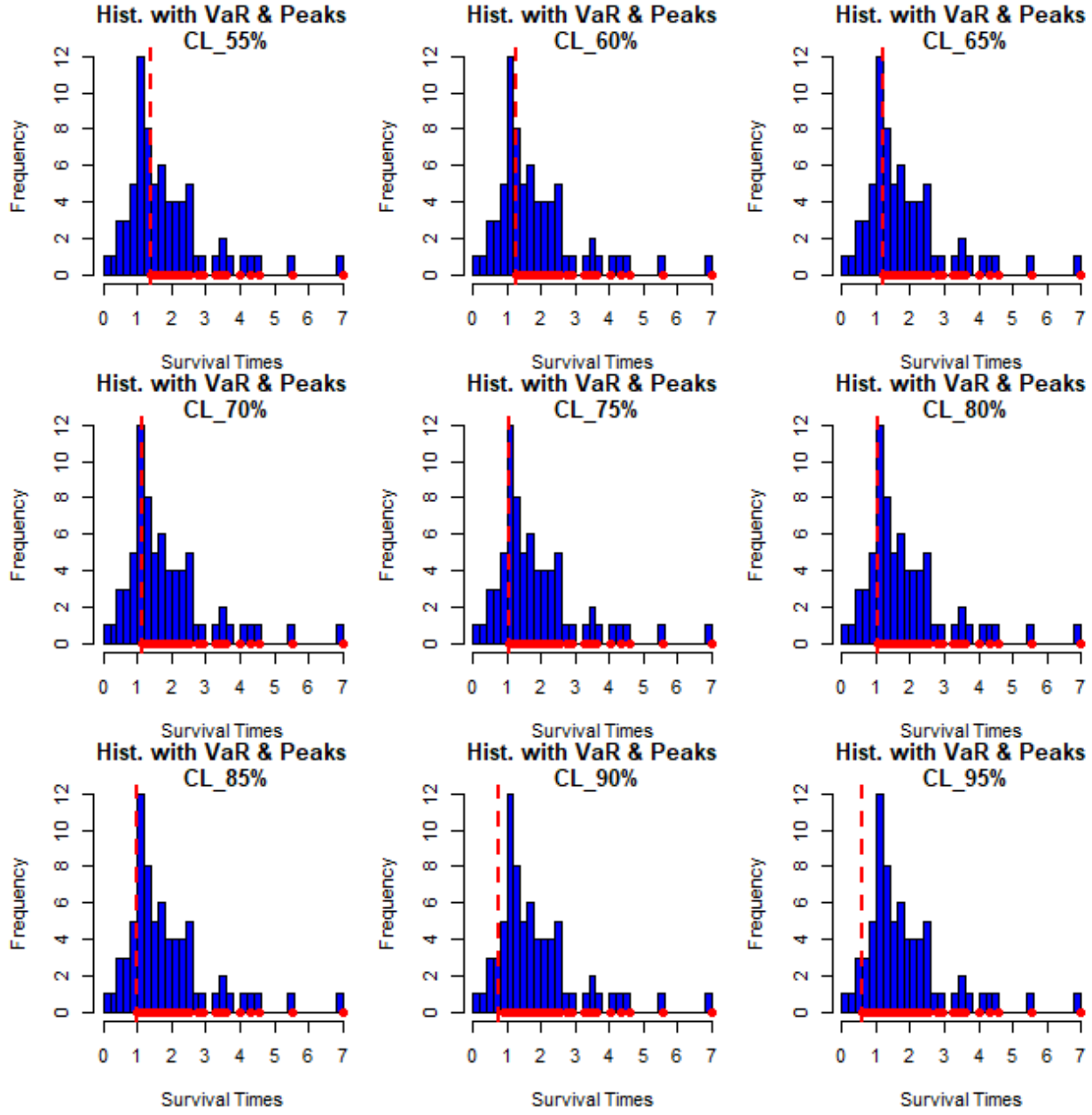

Figure 9: Histograms with VaR and related peaks for the survival times.

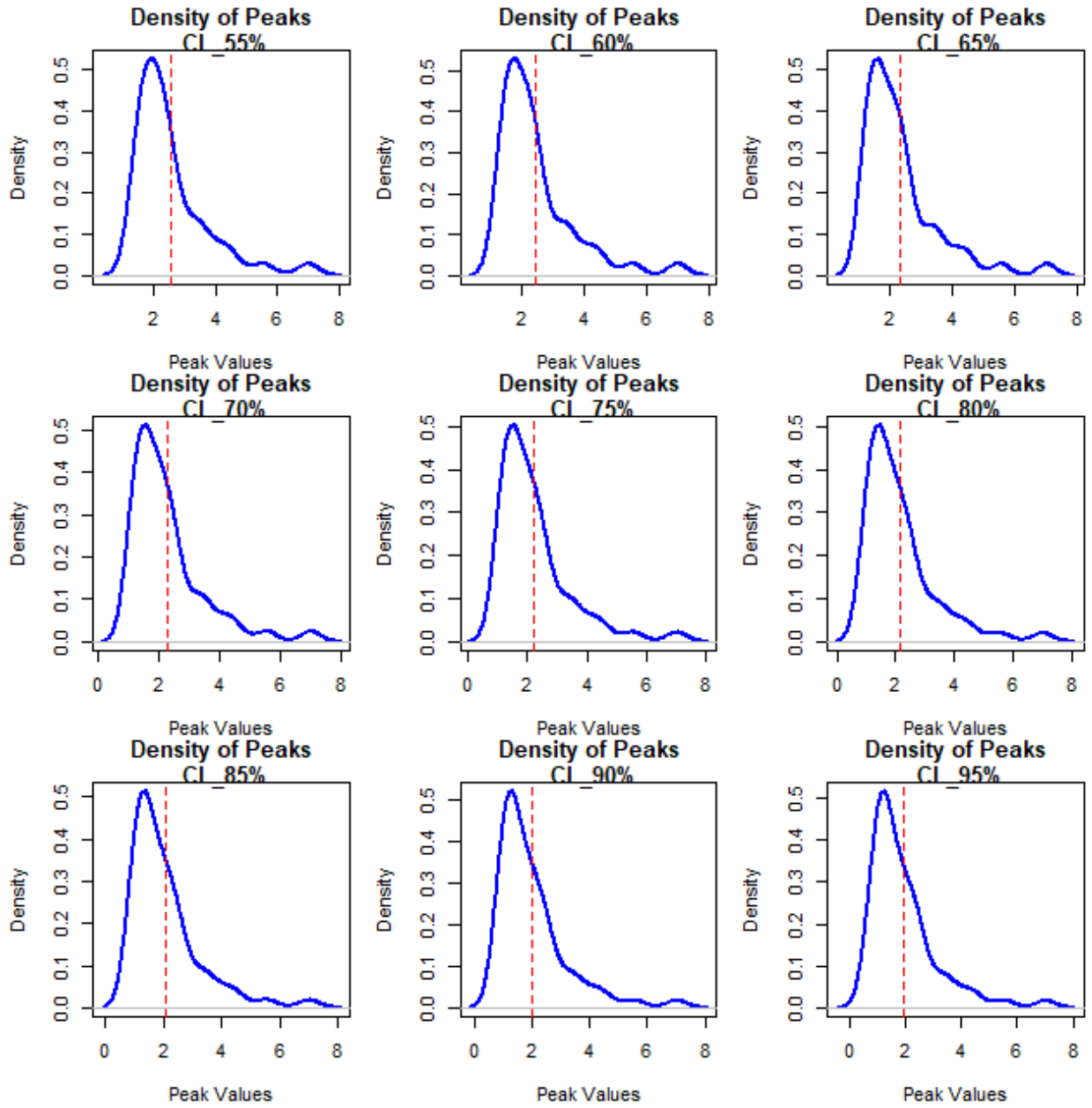

Figure 10: Kernel densities with VaR and related peaks for the survival times.

9. Conclusions, discussion and future points

This paper introduced an innovative extension of the exponential distribution called the extended exponentiated exponential (ExEE), designed to advance reliability and risk analysis through a more nuanced approach. Traditional exponential models, while valuable for their simplicity and effectiveness in modeling time-to-failure and survival times, often fall short in capturing the complex risk profiles associated with extreme events. Our new model addresses this limitation by integrating key insurance risk indicators including the value-at-risk (VaRq), tail mean-variance (TMVq), tail value-at-risk (TVaRq), tail variance (TVq), and maximum excess loss (MELq) to provide a more comprehensive risk assessment framework. These indicators are crucial for understanding the financial ramifications of rare and severe risk events. VaRq offers insights into the maximum expected loss over a specified period at a given confidence level, while TMVq and TVq provide detailed analyses of the variability and potential for extreme outcomes within the distribution's tail. TVaRq focuses on losses beyond specific quantiles, presenting a more thorough view of extreme risk. MELq further refines this analysis by examining the impact of unusually large losses. To rigorously

evaluate these risk indicators, we employ a range of non-Bayesian estimation techniques, including maximum likelihood estimation (MLE), ordinary least squares estimation (OLSE), Anderson-Darling estimation (ADE), right tail Anderson-Darling estimation (RTADE), and left tail Anderson-Darling estimation of the second order (LAD 2). Our methodology involves a detailed simulation study across various sample sizes to assess the robustness and accuracy of these estimation methods. This is followed by an empirical analysis to validate our findings and evaluate the new model's performance. We apply our enhanced model to two real-world reliability data sets to demonstrate its practical applicability. This includes a thorough analysis using both failure (relief) and survival data, which underscores the model's versatility and effectiveness in different scenarios. Our findings provide valuable recommendations for practitioners and researchers in reliability engineering and risk management. We advocate for the adoption of our extended model and the associated risk indicators in both theoretical and practical contexts. This approach promises to offer more precise and actionable insights into risk assessment, particularly in environments characterized by extreme and rare events.

Given that MLE consistently provides relatively high values for VaRq, TVaRq, and MELq across different confidence levels, it should be prioritized for its accuracy in capturing extreme risks. It offers reliable estimates for high confidence levels (90%) and is effective in assessing both typical and extreme failure events. While OLSE provides lower estimates compared to other methods, its simplicity and ease of implementation make it a viable choice for scenarios where computational efficiency is prioritized over precision. This method is particularly useful when data or computational resources are limited. ADE offers robust performance across various confidence levels and provides a good balance between accuracy and computational complexity. It is particularly effective in capturing the behavior of failure times and should be considered for reliability analyses where robustness is key. RTADE is advantageous for modeling the right tail of the distribution, making it suitable for scenarios where extreme failure events are of particular interest. This method's higher values for tail indicators suggest its effectiveness in assessing severe risk scenarios. LAD 2 provides lower estimates for risk indicators but excels in capturing lower tail behaviors with precision. It is recommended for detailed analysis of lower failure rate scenarios and when precise estimation of the lower tail is required.

MLE consistently shows higher values for VaRq, TVaRq, and MELq across different confidence levels (70%, 80%, and 90%), indicating its effectiveness in capturing extreme survival risks. It is recommended for analyses where precision in high-confidence scenarios is crucial, especially when dealing with severe risk events. OLSE provides a simpler and more straightforward approach, with reasonably accurate estimates for KRIs under survival times. While it offers lower values compared to MLE, its ease of use makes it suitable for scenarios where computational efficiency and simplicity are prioritized over precision. ADE offers a balanced performance across various confidence levels, making it a robust choice for survival time analysis. It is effective in providing accurate risk assessments and is recommended for situations where reliability and consistency in estimation are required. RTADE is particularly useful for modeling the right tail of the survival time distribution. Its higher values for indicators suggest its strength in assessing extreme survival risks and should be used when focusing on scenarios involving very long survival times. LAD 2 excels in providing precise estimates for lower tail behaviors. It is recommended for detailed analysis of scenarios where precise estimation of lower tail survival times is critical, even though it provides slightly lower values compared to other methods.

Finaly, the PORT-VaRq analysis for failure survival times provided us some valuable insights into the behavior of extreme survival events across varying confidence levels. As the confidence level increases, the VaRq threshold decreases, capturing a progressively larger number of extreme survival times, which are essential for understanding long-term reliability and risk. The steady increase in the number of peaks above VaRq, from 40 at CL of 55% to 68 at CL of 95%, highlights the growing sensitivity to rare, extreme survival events as the threshold lowers. This trend aligns with expectations in reliability and risk analysis, where lower VaRq thresholds allow for a more comprehensive assessment of tail risks. This analysis is crucial for predicting extreme survival scenarios in various fields such as medical research, engineering reliability, and environmental risk management. It emphasizes the importance of considering extreme values in system design and decision-making, particularly for systems where failure or survival is influenced by complex factors. By providing a clearer picture of tail risks, the PORT-VaRq methodology enhances the reliability of survival models, helping stakeholders make more informed decisions regarding maintenance, safety protocols, and resource allocation. Ultimately, this approach improves the understanding and management of long-term survival risks, ensuring better preparedness for rare but high-impact events.

Future works could be allocated to study this new exponential model in many applied directions such as copula types and reliability applications (see Yousof et al. (2021b), Mansour et al. (2020a,b,c,d,f); Salah et al. (2020), Abiad et al. (2025)). Accelerated life testing (Abonongo et al. (2025)), more characterization theories (Abouelmagd et al. (2019) and Yousof et al. (2022)). Amputated life-testing (Ahmed et al. (2024)), single acceptance sampling plan (Ahmed et al. (2022)), different real data and extreme value data (Ali et al. (2022) and et al. (2025)). Rao-Robson-Nikulin goodness-of-fit test statistic (Yadav et al. (2020) , Ibrahim et al. (2019; 2021; 2020; 2022a,b; 2023; 2025a,b); Goual et al. (2019, 2020,2022); Goual and Yousof (2020); Yousof et al. (2022); Salem et al. (2023), Shehata et al. (2024b), AlKhayyat et al. (2025)). Bayesian and non-Bayesian distributional validation (Emam et al. (2023a)). Bayesian inference in accelerated testing (Hashem et al. (2024)). More risk application (Shrahili et al. (2021), Rasekhi et al. (2022), Korkmaz et al. (2018a), Hashempour et al. (2024a,b)). Missing data analysis in epidemiological research (Javadi et al. (2024)). Some new frailty models based on Loubna et al. (2024) and Teghri et al. (2024). Consistency issues in skew random fields with applications (Taghipour et al. (2025)). Some new modified Chi-square type test for right censored validation with applications (see Yousof et al. (2021a)). A novel discrete model for the actuarial studies based on our new exponential model (Aboraya et al. (2020), Ibrahim et al. (2021), Yousof et al. (2020; 2021c; 2021e), Chesneau et al. (2022), Emam et al. (2023b) and Yousof et al. (2024c,d)). Value-at-risk analysis for the historical insurance claims (Yousof et al. (2025)).

References

1. Abiad, M., Alsadat, N., Abd El-Raouf, M. M., Yousof, H. M., & Kumar, A. (2025). Different copula types and reliability applications for a new fisk probability model. Alexandria Engineering Journal, 110, 512-526.
2. Abonongo, J., Abonongo, A. I. L., Aljadani, A., Mansour, M. M., & Yousof, H. M. (2025). Accelerated failure model with empirical analysis and application to colon cancer data: Testing and validation. Alexandria Engineering Journal, 113, 391-408.
3. Aboraya, M., M. Yousof, H. M., Hamedani, G. G., & Ibrahim, M. (2020). A new family of discrete distributions with mathematical properties, characterizations, Bayesian and non-Bayesian estimation methods. Mathematics, 8, 1648.
4. Abouelmagd, T. H. M., Hamed, M. S., Hamedani, G. G., Ali, M. M., Goual, H., Korkmaz, M. C., & Yousof, H. M. (2019). The zero truncated Poisson Burr X family of distributions with properties, characterizations, applications, and validation test. Journal of Nonlinear Sciences and Applications, 12(5), 314-336.
5. Ahmed, B., Ali, M. M. and Yousof, H. M. (2022). A Novel G Family for Single Acceptance Sampling Plan with Application in Quality and Risk Decisions, Annals of Data Science, 10.1007/s40745-022-00451-3
6. Ahmed, B., Hamedani, G. G., Mekiso, G. T., Tashkandy, Y. A., Bakr, M. E., Hussam, E., & Yousof, H. M. (2024). Amputated life-testing based on extended Dagum percentiles for type of group inspection plans: optimal sample sizes, termination time ratios analysis. *Scientific Reports*, *14*(1), 24144.
7. Ali, M. M., Ali, I., Yousof, H. M. and Ibrahim, M. (2022). G Families of Probability Distributions: Theory and Practices. CRC Press, Taylor & Francis Group.
8. Ali, M. M., Imon, R., Ali, I. and Yousof, H. M. (2025). Statistical Outliers and Related Topics. CRC Press, Taylor & Francis Group.
9. Alizadeh, M., Afshari, M., Contreras-Reyes, J. E., Mazarei, D., & Yousof, H. M. (2024). The Extended Gompertz Model: Applications, Mean of Order P Assessment and Statistical Threshold Risk Analysis Based on Extreme Stresses Data. IEEE Transactions on Reliability, doi: 10.1109/TR.2024.3425278.
10. Alizadeh, M., Afshari, M., Cordeiro, G. M., Ramaki, Z., Contreras-Reyes, J. E., Dirnik, F., & Yousof, H. M. (2025). A New Weighted Lindley Model with Applications to Extreme Historical Insurance Claims. Stats, 8(1), 8.
11. Alizadeh, M., Afshari, M., Ranjbar, V., Merovci, F. and Yousof, H. M. (2023a). A novel XGamma extension: applications and actuarial risk analysis under the reinsurance data. São Paulo Journal of Mathematical Sciences, 1-31.
12. Alizadeh, M., Afshari, M., Ranjbar, V., Merovci, F. and Yousof, H. M. (2023b). A novel XGamma extension: applications and actuarial risk analysis under the reinsurance data. São Paulo Journal of Mathematical Sciences, 1-31.
13. Alizadeh, M., Ghosh, I., Yousof, H. M., Rasekhi, M., & Hamedani, G. G. (2017). The generalized odd generalized exponential family of distributions: properties, characterizations and applications. Journal of Data Science, 15(3), 443-465.
14. Aljadani, A., Mansour, M. M., & Yousof, H. M. (2024a). A Novel Model for Finance and Reliability Applications: Theory, Practices and Financial Peaks Over a Random Threshold Value-at-Risk Analysis. Pakistan Journal of Statistics and Operation Research, 20(3), 489-515. https://doi.org/10.18187/pjsor.v20i3.4439

15. Aljadani, A., Mansour, M. M., & Yousof, H. M. (2024b). A Novel Model for Finance and Reliability Applications: Theory, Practices and Financial Peaks Over a Random Threshold Value-at-Risk Analysis. Pakistan Journal of Statistics and Operation Research, 20(3), 489-515. https://doi.org/10.18187/pjsor.v20i3.4439
16. AlKhayyat, S. L., Haitham M. Yousof, Hafida Goual, Hamida, T., Hamed, M. S., Hiba, A., & Mohamed Ibrahim. (2025). Rao-Robson-Nikulin Goodness-of-fit Test Statistic for Censored and Uncensored Real Data with Classical and Bayesian Estimation. Statistics, Optimization & Information Computing. https://doi.org/10.19139/soic-2310-5070-1710
17. Aslam, M., Kundu, D., Ahmad, M. (2010). Time truncated acceptance sampling plans for generalized exponential distribution. J. Appl. Stat. 37, 555-566.
18. Bain, L. (2017). Statistical analysis of reliability and life-testing models: theory and methods. Routledge.
19. Bhatti, F. A., Hamedani, G. G., Yousof, H. M., & Ali, A. (2022). On the Burr III-Moment Exponential Distribution. Thailand statistician, Vol. 20 No. 3, 615-635.
20. Chesneau, C., Yousof, H. M., Hamedani, G., & Ibrahim, M. (2022). A New One-parameter Discrete Distribution: The Discrete Inverse Burr Distribution: Characterizations, Properties, Applications, Bayesian and Non-Bayesian Estimations. Statistics, Optimization & Information Computing, 10(2), 352-371.
21. Das, J., Hazarika, P. J., Alizadeh, M., Contreras-Reyes, J. E., Mohammad, H. H., & Yousof, H. M. (2025). Economic Peaks and Value-at-Risk Analysis: A Novel Approach Using the Laplace Distribution for House Prices. Mathematical and Computational Applications, 30(1), 4.
22. Elbatal, I., Diab, L. S., Ghorbal, A. B., Yousof, H. M., Elgarhy, M. and Ali, E. I. (2024). A new losses (revenues) probability model with entropy analysis, applications and case studies for value-at-risk modeling and mean of order-P analysis. AIMS Mathematics, 9(3), 7169-7211.
23. Eliwa, M. S., El-Morshedy, M. and Yousof, H. M. (2022). A Discrete Exponential Generalized-G Family of Distributions: Properties with Bayesian and Non-Bayesian Estimators to Model Medical, Engineering and Agriculture Data. Mathematics, 10, 3348. https://doi.org/10.3390/math10183348
24. Emam, W., Tashkandy, Y., Goual, H., Hamida, T., Hiba, A., Ali, M. M., ... & Ibrahim, M. (2023a). A new one-parameter distribution for right censored bayesian and non-bayesian distributional validation under various estimation methods. *Mathematics*, *11*(4), 897.
25. Emam, W., Tashkandy, Y., Hamedani, G. G., Shehab, M. A., Ibrahim, M., & Yousof, H. M. (2023b). A Novel Discrete Generator with Modeling Engineering, Agricultural and Medical Count and Zero-Inflated Real Data with Bayesian, and Non-Bayesian Inference. Mathematics, 11(5), 1125.
26. Furman, E., & Landsman, Z. (2006). Tail variance premium with applications for elliptical portfolio of risks. ASTIN Bulletin: The Journal of the IAA, 36(2), 433-462.
27. Glänzel, W., A characterization theorem based on truncated moments and its application to some distribution families, Mathematical Statistics and Probability Theory (Bad Tatzmannsdorf, 1986), Vol. B, Reidel, Dordrecht, 1987, 75-84.
28. Glänzel, W., Some consequences of a characterization theorem based on truncated moments, Statistics: A Journal of Theoretical and Applied Statistics, 21 (4), 1990, 613-618.
29. Goual, H., & Yousof, H. M. (2020). Validation of Burr XII inverse Rayleigh model via a modified chi-squared goodness-of-fit test. Journal of Applied Statistics, 47(3), 393-423.
30. Goual, H., Hamida, T., Hiba, A., Hamedani, G.G., Ibrahim, M. and Yousof, H. M. (2022). Bayesian and Non-Bayesian Distributional Validations under Censored and Uncensored Schemes with Characterizations and Applications
31. Goual, H., Yousof, H. M., & Ali, M. M. (2019). Validation of the odd Lindley exponentiated exponential by a modified goodness of fit test with applications to censored and complete data. Pakistan Journal of Statistics and Operation Research, 15(3), 745-771.
32. Goual, H., Yousof, H. M., & Ali, M. M. (2019). Validation of the odd Lindley exponentiated exponential by a modified goodness of fit test with applications to censored and complete data. Pakistan Journal of Statistics and Operation Research, 15(3), 745-771.
33. Goual, H., Yousof, H. M., & Ali, M. M. (2020). Lomax inverse Weibull model: properties, applications, and a modified Chi-squared goodness-of-fit test for validation. Journal of Nonlinear Sciences & Applications (JNSA), 13(6), 330-353.
34. Hamed, M. S., Cordeiro, G. M. and Yousof, H. M. (2022). A New Compound Lomax Model: Properties, Copulas, Modeling and Risk Analysis Utilizing the Negatively Skewed Insurance Claims Data. Pakistan Journal of Statistics and Operation Research, 18(3), 601-631. https://doi.org/10.18187/pjsor.v18i3.3652

35. Hamedani, G. G., Goual, H., Emam, W., Tashkandy, Y., Ahmad Bhatti, F., Ibrahim, M. and Yousof, H. M. (2023). A new right-skewed one-parameter distribution with mathematical characterizations, distributional validation, and actuarial risk analysis, with applications. Symmetry, 15(7), 1297.
36. Hamedani, G. G., Rasekhi, M., Najibi, S., Yousof, H. M., & Alizadeh, M. (2019). Type II general exponential class of distributions. Pakistan Journal of Statistics and Operation Research, 15(2), 503-523.
37. Hamedani, G. G., Yousof, H. M., Rasekhi, M., Alizadeh, M. and Najibi, S. M., (2018). Type I general exponential class of distributions. Pakistan Journal of Statistics and Operation Research, 14(1), 39-55.
38. Hashem, A. F., Alotaibi, N., Alyami, S. A., Abdelkawy, M. A., Elgawad, M. A. A., Yousof, H. M., & Abdel-Hamid, A. H. (2024). Utilizing Bayesian inference in accelerated testing models under constant stress via ordered ranked set sampling and hybrid censoring with practical validation. Scientific Reports, 14(1), 14406.
39. Hashempour, M., Alizadeh, M. and Yousof, H. M. (2023). A New Lindley Extension: Estimation, Risk Assessment and Analysis Under Bimodal Right Skewed Precipitation Data. Annals of Data Science, 1-40.
40. Hashempour, M., Alizadeh, M., & Yousof, H. (2024a). The Weighted Xgamma Model: Estimation, Risk Analysis and Applications. Statistics, Optimization & Information Computing, 12(6), 1573-1600.
41. Hashempour, M., Alizadeh, M., & Yousof, H. M. (2024b). A new Lindley extension: estimation, risk assessment and analysis under bimodal right skewed precipitation data. Annals of Data Science, 11(6), 1919-1958.
42. Ibrahim, M., Ali, M. M., & Yousof, H. M. (2021). The discrete analogue of the Weibull G family: properties, different applications, Bayesian and non-Bayesian estimation methods. Annals of Data Science, 1-38.
43. Ibrahim, M., Ali, M. M., Goual, H., & Yousof, H. (2022a). The Double Burr Type XII Model: Censored and Uncensored Validation Using a New Nikulin-Rao-Robson Goodness-of-Fit Test with Bayesian and Non-Bayesian Estimation Methods. Pakistan Journal of Statistics and Operation Research, 18(4), 901-927. https://doi.org/10.18187/pjsor.v18i4.3600
44. Ibrahim, M., Altun, E., Goual, H., and Yousof, H. M. (2020). Modified goodness-of-fit type test for censored validation under a new Burr type XII distribution with different methods of estimation and regression modeling. Eurasian Bulletin of Mathematics, 3(3), 162-182.
45. Ibrahim, M., Ansari, S. I., Al-Nefaie, A. H., & Yousof, H. M. (2025a). A New Version of the Inverse Weibull Model with Properties, Applications and Different Methods of Estimation. Statistics, Optimization & Information Computing, 13(3), 1120-1143. https://doi.org/10.19139/soic-2310-5070-1658
46. Ibrahim, M., Butt, N. S., Al-Nefaie, A. H., Hamedani, G. G., Yousof, H. M., & Mahmoud, A. S. (2025b). An Extended Discrete Model for Actuarial Data and Value at Risk Analysis: Properties, Applications and Risk Analysis under Financial Automobile Claims Data. Statistics, Optimization & Information Computing, 13(1), 27-46.
47. Ibrahim, M., Hamedani, G. G., Butt, N. S. and Yousof, H. M. (2022b). Expanding the Nadarajah Haghighi Model: Copula, Censored and Uncensored Validation, Characterizations and Applications. Pakistan Journal of Statistics and Operation Research, 18(3), 537-553. https://doi.org/10.18187/pjsor.v18i3.3420
48. Ibrahim, M., Yadav, A. S., Yousof, H. M., Goual, H., & Hamedani, G. G. (2019). A new extension of Lindley distribution: modified validation test, characterizations and different methods of estimation. Communications for Statistical Applications and Methods, 26(5), 473-495.
49. Ibrahim, M.; Emam, W.; Tashkandy, Y.; Ali, M.M.; Yousof, H.M. (2023). Bayesian and Non-Bayesian Risk Analysis and Assessment under Left-Skewed Insurance Data and a Novel Compound Reciprocal Rayleigh Extension. Mathematics 2023, 11, 1593. https://doi.org/10.3390/ math11071593
50. Ibrahim. M., Aidi, K., Ali, M. M. and Yousof, H. M. (2021). The Exponential Generalized Log-Logistic Model: Bagdonavičius-Nikulin test for Validation and Non-Bayesian Estimation Methods. Communications for Statistical Applications and Methods, 29(1), 681–705.
51. Javadi, S., Saber, M. M., Taghipour, M., Aljadani, A., Mansour, M. M., Hamed, M.S., and Yousof, H. M. (2024). A comparative analysis of parametric and tree-based imputation techniques for missing data in epidemiological research, Journal of Applied Probability and Statistics, 19(3), 99-113.
52. Khan, M. I., Aljadani, A., Mansour, M. M., Abd Elrazik, E. M., Hamedani, G. G., Yousof, H. M., & Shehata, W. A. (2024). A New Heavy-Tailed Lomax Model with Characterizations, Applications, Peaks Over Random Threshold Value-at-Risk, and the Mean-of-Order-P Analysis. Journal of Mathematics, 2024(1), 5329529.
53. Khedr, A. M., Nofal, Z. M., El Gebaly, Y. M. and Yousof, H. M. (2023). A Novel Family of Compound Probability Distributions: Properties, Copulas, Risk Analysis and Assessment under a Reinsurance Revenues Data Set. Thailand Statistician, forthcoming.
54. Korkmaz, M. Ç., & Yousof, H. M. (2017). The one-parameter odd Lindley exponential model: mathematical properties and applications. Stochastics and Quality Control, 32(1), 25-35.

55. Korkmaz, M. Ç., Altun, E., Yousof, H. M., Afify, A. Z. and Nadarajah, S. (2018). The Burr X Pareto Distribution: Properties, Applications and VaR Estimation. Journal of Risk and Financial Management, 11(1), 1.
56. Korkmaz, M. Ç., Yousof, H. M., & Hamedani, G. G. (2018). The exponential Lindley odd log-logistic-G family: properties, characterizations and applications. Journal of Statistical Theory and Applications, 17(3), 554-571.
57. Kundu, D. and Pradhan, B. (2009). Bayesian inference and life testing plans for generalized exponential distribution. Sci. China Ser. A, Math. 52, 1373-1388.
58. Landsman, Z. (2010). On the tail mean-variance optimal portfolio selection. Insurance: Mathematics and Economics, 46(3), 547-553.
59. Loubna, H., Goual, H., Alghamdi, F. M., Mustafa, M. S., Tekle Mekiso, G., Ali, M. M., ... & Yousof, H. M. (2024). The quasi-xgamma frailty model with survival analysis under heterogeneity problem, validation testing, and risk analysis for emergency care data. Scientific Reports, 14(1), 8973.
60. Mansour, M. M., Butt, N. S., Ansari, S. I., Yousof, H. M., Ali, M. M., & Ibrahim, M. (2020a). A new exponentiated Weibull distribution's extension: copula, mathematical properties and applications. Contributions to Mathematics, 1 (2020) 57–66. DOI: 10.47443/cm.2020.0018
61. Mansour, M. M., Butt, N. S., Yousof, H. M., Ansari, S. I., & Ibrahim, M. (2020b). A Generalization of Reciprocal Exponential Model: Clayton Copula, Statistical Properties and Modeling Skewed and Symmetric Real Data Sets. Pakistan Journal of Statistics and Operation Research, 16(2), 373-386.
62. Mansour, M. M., Ibrahim, M., Aidi, K., Butt, N. S., Ali, M. M., Yousof, H. M., & Hamed, M. S. (2020c). A New Log-Logistic Lifetime Model with Mathematical Properties, Copula, Modified Goodness-of-Fit Test for Validation and Real Data Modeling. Mathematics, 8(9), 1508.
63. Mansour, M., Korkmaz, M. Ç., Ali, M. M., Yousof, H. M., Ansari, S. I., & Ibrahim, M. (2020d). A generalization of the exponentiated Weibull model with properties, Copula and application. Eurasian Bulletin of Mathematics, 3(2), 84-102.
64. Mansour, M., Rasekhi, M., Ibrahim, M., Aidi, K., Yousof, H. M., & Elrazik, E. A. (2020e). A New Parametric Life Distribution with Modified Bagdonavičius–Nikulin Goodness-of-Fit Test for Censored Validation, Properties, Applications, and Different Estimation Methods. Entropy, 22(5), 592.
65. Mansour, M., Yousof, H. M., Shehata, W. A. M., & Ibrahim, M. (2020f). A new two parameter Burr XII distribution: properties, copula, different estimation methods and modeling acute bone cancer data. Journal of Nonlinear Science and Applications, 13(5), 223-238.
66. McNeil, A. J., & Saladin, T. (1997). The peaks over thresholds method for estimating high quantiles of loss distributions. In Proceedings of 28th international ASTIN Colloquium (Vol. 23, P. 43).
67. Minkah, R., de Wet, T., Ghosh, A., & Yousof, H. M. (2023). Robust extreme quantile estimation for Pareto-type tails through an exponential regression model. Communications for Statistical Applications and Methods, 30(6), 531-550.
68. Mohamed, H. S., Cordeiro, G. M., Minkah, R., Yousof, H. M., & Ibrahim, M. (2024). A size-of-loss model for the negatively skewed financial claims data: applications, risk analysis using different methods and statistical forecasting. Journal of Applied Statistics, 51(2), 348-369.
69. Rasekhi, M., Altun, E., Alizadeh, M. and Yousof, H. M. (2022). The Odd Log-Logistic Weibull-G Family of Distributions with Regression and Financial Risk Models. Journal of the Operations Research Society of China, 10(1), 133-158.
70. Saber, M. M. Marwa M. Mohie El-Din and Yousof, H. M. (2022). Reliability estimation for the remained stress-strength model under the generalized exponential lifetime distribution, Journal of Probability and Statistics, 2021, 1-10.
71. Salah, M. M., El-Morshedy, M., Eliwa, M. S. and Yousof, H. M. (2020). Expanded Fréchet Model: Mathematical Properties, Copula, Different Estimation Methods, Applications and Validation Testing. Mathematics, 8(11), 1949.
72. Salem, M., Emam, W., Tashkandy, Y., Ibrahim, M., Ali, M. M., Goual, H. and Yousof, H. M. (2023). A new lomax extension: Properties, risk analysis, censored and complete goodness-of-fit validation testing under left-skewed insurance, reliability and medical data. Symmetry, 15(7), 1356.
73. Shehata, W. A. M., Aljadani, A., Mansour, M. M., Alrweili, H., Hamed, M. S., & Yousof, H. M. (2024a). A Novel Reciprocal-Weibull Model for Extreme Reliability Data: Statistical Properties, Reliability Applications, Reliability PORT-VaR and Mean of Order P Risk Analysis. Pakistan Journal of Statistics and Operation Research, 20(4), 693-718. https://doi.org/10.18187/pjsor.v20i4.4302
74. Shehata, W. A., Goual, H., Hamida, T., Hiba, A., Hamedani, G. G., Al-Nefaie, A. H., Ibrahim, M., Butt, N. S., Osman, R. M. A., and Yousof, H. M. (2024b). Censored and Uncensored Nikulin-Rao-Robson Distributional

Validation: Characterizations, Classical and Bayesian estimation with Censored and Uncensored Applications. Pakistan Journal of Statistics and Operation Research, 20(1), 11-35.
75. Shrahili, M.; Elbatal, I. and Yousof, H. M. Asymmetric Density for Risk Claim-Size Data: Prediction and Bimodal Data Applications. Symmetry 2021, 13, 2357.
76. Shrahili, M.; Elbatal, I. and Yousof, H. M. Asymmetric Density for Risk Claim-Size Data: Prediction and Bimodal Data Applications. Symmetry 2021, 13, 2357. https://doi.org/10.3390/sym13122357
77. Taghipour, M., Saber, M. M., Khan, M. I., Hamed, M. S. & Yousof, H. M. (2025). Consistency Issues in Skew Random Fields: Investigating Proposed Alternatives and Identifying Persisting Problems. Pakistan Journal of Statistics and Operation Research, 21(1), 33-37. https://doi.org/10.18187/pjsor.v21i1.4577
78. Teghri, S., Goual, H., Loubna, H., Butt, N. S., Khedr, A. M., Yousof, H. M., ... & Salem, M. (2024). A New Two-Parameters Lindley-Frailty Model: Censored and Uncensored Schemes under Different Baseline Models: Applications, Assessments, Censored and Uncensored Validation Testing. Pakistan Journal of Statistics and Operation Research, 109-138.
79. Yadav, A. S., Altun, E., & Yousof, H. M. (2021). Burr-Hatke Exponential Distribution: A Decreasing Failure Rate Model, Statistical Inference and Applications. Annals of Data Science, 8(2), 241-260.
80. Yadav, A. S., Goual, H., Alotaibi, R. M., Rezk, H., Ali, M. M., & Yousof, H. M. (2020). Validation of the Topp-Leone-Lomax model via a modified Nikulin-Rao-Robson goodness-of-fit test with different methods of estimation. Symmetry, 12(1), 57.
81. Yadav, A. S., Shukla, S., Goual, H., Saha, M. and Yousof, H. M. (2022). Validation of xgamma exponential model via Nikulin-Rao-Robson goodness-of- fit test under complete and censored sample with different methods of estimation. Statistics, Optimization & Information Computing, 10(2), 457-483.
82. Yousof, H. M., Aidi, K., Hamedani, G. G and Ibrahim, M. (2021a). A new parametric lifetime distribution with modified Chi-square type test for right censored validation, characterizations and different estimation methods. Pakistan Journal of Statistics and Operation Research, 17(2), 399-425.
83. Yousof, H. M., Ali, E. I. A., Aidi, K., Butt, N. S., Saber, M. M., Al-Nefaie, A. H., Aljadani, A., Mansour, M. M., Hamed, M. S., & Ibrahim, M. (2025). The Statistical Distributional Validation under a Novel Generalized Gamma Distribution with Value-at-Risk Analysis for the Historical Claims, Censored and Uncensored Real-life Applications. Pakistan Journal of Statistics and Operation Research, 21(1), 51-69. https://doi.org/10.18187/pjsor.v21i1.4534
84. Yousof, H. M., Ali, M. M., Aidi, K., Ibrahim, M. (2023a). The modified Bagdonavičius-Nikulin goodness-of-fit test statistic for the right censored distributional validation with applications in medicine and reliability. Statistics in Transition New Series, 24(4), 1-18.
85. Yousof, H. M., Ali, M. M., Goual, H. and Ibrahim. M. (2021b). A new reciprocal Rayleigh extension: properties, copulas, different methods of estimation and modified right censored test for validation, Statistics in Transition New Series, 23(3), 1-23.
86. Yousof, H. M., Ali, M. M., Hamedani, G. G., Aidi, K. & Ibrahim, M. (2022). A new lifetime distribution with properties, characterizations, validation testing, different estimation methods. Statistics, Optimization & Information Computing, 10(2), 519-547.
87. Yousof, H. M., Aljadani, A., Mansour, M. M., & Abd Elrazik, E. M. (2024a). A New Pareto Model: Risk Application, Reliability MOOP and PORT Value-at-Risk Analysis. Pakistan Journal of Statistics and Operation Research, 20(3), 383-407. https://doi.org/10.18187/pjsor.v20i3.4151
88. Yousof, H. M., Aljadani, A., Mansour, M. M., & Abd Elrazik, E. M. (2024b). A New Pareto Model: Risk Application, Reliability MOOP and PORT Value-at-Risk Analysis. Pakistan Journal of Statistics and Operation Research, 20(3), 383-407. https://doi.org/10.18187/pjsor.v20i3.4151
89. Yousof, H. M., Al-Nefaie, A. H., Butt, N. S., Hamedani, G., Alrweili, H., Aljadani, A., Mansour, M. M., Hamed, M. S., & Ibrahim, M. (2024c). A New Discrete Generator with Mathematical Characterization, Properties, Count Statistical Modeling and Inference with Applications to Reliability, Medicine, Agriculture, and Biology Data. Pakistan Journal of Statistics and Operation Research, 20(4), 745-770. https://doi.org/10.18187/pjsor.v20i4.4616
90. Yousof, H. M., Ansari, S. I., Tashkandy, Y., Emam, W., Ali, M. M., Ibrahim, M., Alkhayyat, S. L. (2023b). Risk Analysis and Estimation of a Bimodal Heavy-Tailed Burr XII Model in Insurance Data: Exploring Multiple Methods and Applications. Mathematics. 2023; 11(9):2179. https://doi.org/10.3390/math11092179
91. Yousof, H. M., Chesneau, C., Hamedani, G., & Ibrahim, M. (2021c). A New Discrete Distribution: Properties, Characterizations, Modeling Real Count Data, Bayesian and Non-Bayesian Estimations. Statistica, 81(2), 135-162.

92. Yousof, H. M., Goual, H., Emam, W., Tashkandy, Y., Alizadeh, M., Ali, M. M., & Ibrahim, M. (2023c). An Alternative Model for Describing the Reliability Data: Applications, Assessment, and Goodness-of-Fit Validation Testing. Mathematics, 11(6), 1308.
93. Yousof, H. M., Goual, H., Hamida, T., Hiba, A., Hamedani, G.G. and Ibrahim, M. (2022). Censored and Uncensored Nikulin-Rao-Robson Distributional Validation: Characterizations, Classical and Bayesian estimation with Applications.
94. Yousof, H. M., Goual, H., Khaoula, M. K., Hamedani, G. G., Al-Aefaie, A. H., Ibrahim, M., ... & Salem, M. (2023d). A novel accelerated failure time model: Characterizations, validation testing, different estimation methods and applications in engineering and medicine. Pakistan Journal of Statistics and Operation Research, 19(4), 691-717.
95. Yousof, H. M., Hamedani, G. G. and Ibrahim, M. (2020). The Discrete Weibull Generalized Family: Characterization, Applications, Bayesian and Non-Bayesian Estimation Methods. Communications in Statistics - Theory and Method. Submitted.
96. Yousof, H. M., Saber, M. M., Al-Nefaie, A. H., Butt, N. S., Ibrahim, M. and Alkhayyat, S. L. (2024d). A discrete claims-model for the inflated and over-dispersed automobile claims frequencies data: Applications and actuarial risk analysis. Pakistan Journal of Statistics and Operation Research, 261-284.
97. Yousof, H. M., Saber, M. M., Al-Nefaie, A. H., Butt, N. S., Ibrahim, M., & Alkhayyat, S. L. (2024e). A discrete claims-model for the inflated and over-dispersed automobile claims frequencies data: Applications and actuarial risk analysis. Pakistan Journal of Statistics and Operation Research, 20(2), 261-284.
98. Yousof, H.M.; Emam, W.; Tashkandy, Y.; Ali, M.M.; Minkah, R.; Ibrahim, M. (2023e). A Novel Model for Quantitative Risk Assessment under Claim-Size Data with Bimodal and Symmetric Data Modeling. Mathematics 2023, 11, 1284. https://doi.org/10.3390/math11061284
99. Yousof, H.M.; Tashkandy, Y.; Emam, W.; Ali, M.M.; Ibrahim, M. (2023f). A New Reciprocal Weibull Extension for Modeling Extreme Values with Risk Analysis under Insurance Data. Mathematics 2023, 11, 966. https://doi.org/10.3390/ math11040966
100. Zheng, G. (2002). On the fisher information matrix in type II censored data from the exponentiated exponential family. Biom. J. 44, 353-357.
101. Zheng, G. and Park, S. (2004). A note on time savings in censored life testing. J. Stat. Plan. Inference 124, 289-300.